ISOMERIZATION REACTION SURFACES: QUANTUM MECHANICAL STUDIES OF TRIPLET C_2H_2, SINGLET AIHO AND SINGLET C_2H_2O

George Roger Vacek

REPORT DOCUMENTATION PAGE

Form Approved
OMB No. 0704-0188

1. AGENCY USE ONLY (Leave Blank)	2. REPORT DATE	3. REPORT TYPE AND DATES COVERED
	1995	Final

4. TITLE AND SUBTITLE
Isomerization Reaction Surfaces: Quantum Mechanical Studies of Triplet C2H2, Singlet A1HO and Singlet C2H2O

5. FUNDING NUMBERS

6. AUTHORS
George Roger Vacek

7. PERFORMING ORGANIZATION NAME(S) AND ADDRESS(ES)
The University of Georgia

AFRL-SR-BL-TR-98-
0023

9. SPONSORING/MONITORING AGENCY NAME(S) AND ADDRESS(ES)
AFOSR/NI
110 Duncan Avenue, Room B-115
Bolling Air Force Base, DC 20332-8080

10. SPONSORING/MONITORING AGENCY REPORT NUMBER

11. SUPPLEMENTARY NOTES

12a. DISTRIBUTION AVAILABILITY STATEMENT
Approved for Public Release

12b. DISTRIBUTION CODE

13. ABSTRACT *(Maximum 200 words)*
See attached.

14. SUBJECT TERMS

15. NUMBER OF PAGES

16. PRICE CODE

17. SECURITY CLASSIFICATION OF REPORT	18. SECURITY CLASSIFICATION OF THIS PAGE	19. SECURITY CLASSIFICATION OF ABSTRACT	20. LIMITATION OF ABSTRACT
Unclassified	Unclassified	Unclassified	UL

GEORGE ROGER VACEK

Isomerization Reaction Surfaces: Quantum Mechanical Studies of Triplet C_2H_2, Singlet AlHO and Singlet C_2H_2O

(Under the direction of HENRY F. SCHAEFER, III)

High-level *ab initio* molecular electronic structure theory has been utilized to investigate specific isomerization reaction surfaces including the triplet acetylene and vinylidene potential energy (PE) hypersurface, the $\tilde{X}$ HAlO and $\tilde{X}$ AlOH PE hypersurface and the $\tilde{X}$ oxirene potential energy minima. Basis sets as large as triple zeta plus two sets of polarization functions augmented with higher angular momentum functions [TZ(2df,2pd)] have been utilized in conjunction with correlated methods as sophisticated as the coupled cluster approach including all single, double and perturbative triple excitations [CCSD(T)]. Of particular interest are predictions of the activation energies, zero-point vibrational energy (ZPVE) corrected barriers for rearrangement, of $\tilde{a}\ ^3B_2$ vinylidene to $\tilde{b}\ ^3B_u$ *trans*-bent acetylene and of *cis*-bent $\tilde{a}\ ^3B_2$ acetylene to *trans*-bent $\tilde{b}\ ^3B_u$ acetylene. The physical properties of $\tilde{a}\ ^3B_2$ vinylidene, including the dipole moment, harmonic vibrational frequencies and the infrared intensities, have also been reported. The activation energy and ΔE from $\tilde{X}$ HAlO to $\tilde{X}$ AlOH is predicted. Some molecular properties of HAlO and AlOH in their equilibrium geometries useful for experimental identification purposes are also given. $\tilde{X}$ oxirene has been examined using a large selection of basis sets and a variety of methods of including electron correlation. Different qualitative conclusions regarding the nature of oxirene are reached depending on the choice of basis set and method of electron correlation incorporation. With certain combinations of basis set and theoretical method, the symmetric oxirene structure is found to be a saddle point on the PE surface, while for other combinations oxirene is a local minimum. An analysis is presented for determining the best level of theory for studying the entire oxirene-ketene PE hypersurface.

INDEX WORDS: Acetylene, Vinylidene, Aluminum hydroxide, Ketene, Oxirene,
Ab Initio, Computational Quantum Chemistry

ISOMERIZATION REACTION SURFACES: QUANTUM MECHANICAL STUDIES OF TRIPLET C_2H_2, SINGLET AlHO AND SINGLET C_2H_2O

by

GEORGE ROGER VACEK

B. A. PHYSICS, B. A. MATHEMATICS, University of Wisconsin, 1990.

A Dissertation Submitted to the Graduate Faculty

of the University of Georgia in Partial Fulfillment

of the

Requirements for the Degree

DOCTOR OF PHILOSOPHY

ATHENS, GEORGIA

1995

ISOMERIZATION REACTION SURFACES:

QUANTUM MECHANICAL STUDIES OF TRIPLET C_2H_2,

SINGLET AlHO AND SINGLET C_2H_2O

by

GEORGE ROGER VACEK

Approved:

Henry F. Schaefer III

Major Professor

May 30, 1995

Date

Approved:

Gordhan L. Patel

Graduate Dean

May 31, 1995

Date

For my parents and Nicholas

Acknowledgments

The list of people deserving my thanks for getting this far is so long I won't possibly remember you all. Not only are there those who directly affected me and my research here at the CCQC, but also those who made it possible to survive life here in the South for four years and those who shaped my life from infancy to the point where I consciously decided to get my Ph.D. in theoretical chemistry. If I've forgotten your name or your face, forgive me. I still appreciate everything you've done.

I guess I should start by thanking Brad DeLeeuw for preceding in my footsteps. Among other things he had begun as an undergraduate research fellow in quantum chemistry and told me exciting stories about his work during our long long-distance discussions. Then he returned to the CCQC for graduate school and advised me to apply for the summer program. His promises of many hours of D&D were as much incentive for me to give it a go as the prospect of research. Over the four or so odd years that I've been working in the field, Brad has been the single greatest influence to my life and research.

Next, of course, I must thank Brenda Thiese-Colgrove and Neil Burton (Nil Butron is a pud!) for the great effort they put forth to mentor me through my initial research projects. Not only did they manage to teach me a few things about quantum chemistry, but they also helped me fall in love with the field. So too must I thank Fritz Schaefer, not just for his years spent as my research advisor, but more for his initial leveraging which convinced me to stay with the CCQC rather than going to another school or even another field (such as physics or math).

And the rest of the CCQC is richly deserving in thanks for the wonderful working environment they provided. Dr. Yamaguchi provided me with some of my first project

ideas and showed me how to get alot accomplished. Roger Grev taught me a great deal about chemistry and not a little about everything else. Although I am not certain Curt'n'Ed (Janssen and Seidl) ever took me seriously, they did put up with my puppy-dog enthusiasm, curiosity, and tendency to mess with things. Joseph Fowler is notable for keeping me informed of all of his passions and indirectly, therefore, all of mine. Russ Thomas was the best officemate one could hope for during many long days (and nights) of research. Evan Bolton has added darts and motorcycles to my life and (whether he knew or not) helped me through some of my darkest moments. Thanks to the Germans, Peter Schreiner and Horst Sulzbach; finally some reputations to overshadow mine! The Quantum Trio, Daniel Crawford, Justin Fermann and David Sherrill, helped me with many of the most interesting facets of our field and occasionally with chemical applications. I owe Johnny Galbraith for the music and the salad days. Finally, I would not have been half as successful in graduate school if it hadn't been for the entire CCQC secretarial staff and especially the mothering of Linda Rowe.

This is starting to get long, so I'll have to speed things up, right as I get to the important parts. I wouldn't have survived the South or graduate research without significant support from Bronnie Lee Gilbert, Oh Soon Shropshire, Andrea Grover, Joann Dyson, Dee Dee Vargas, Alacia Hutto, Alison Galbraith, Karen Mehelich, Stacy Schoychid, the Cheema twins (especially Vinita), Rebecca Plante, Diane Sague, Katie Green, Heather Sharpe, Noelle Band, Karen Bradley and Julie Harrison. You have all kept me in touch with reality. I owe my sanity to you.

I also want to mention some of the greater contributions to my personality and education that affected me before my sojourn in Georgia. From my undergraduate days they include Brian Janitschke, Francis Baker III and John Pruitt. From high school, my friends Scott Koehler, Chris Young, John Flaa and Carl Hoeft, and my teachers Darrell Summerfield, Dwayne Heitz, Roland Johnson, John C. Kraus and Steve Bailey. All of you made being a student (among other things) both educational and so enjoyable that I

stuck with it all these years. And, of course, I cannot forget my families (including the Koehlers and the Galbraiths, but most especially the Vaceks) for everything they've done for me.

Finally I'd like to thank whatever-gods-that-be for coffee, without which this document would certainly never have been completed.

if I were to try and describe the sensation
of warm fluid coursing down my throat,
opening wider the chasm of delight within me,
you could not comprehend the pure pleasure I feel
upon accepting this gift from the gods.

-anon

This research was supported in part by a U. S. Department of Defense National Defense Science and Engineering Graduate Fellowship sponsored by the Air Force Office of Scientific Research.

Table of Contents

Acknowledgments iv

Chapter I

Introduction 1

Chapter II

Isomerization reactions on the lowest potential energy hypersurface of triplet vinylidene and triplet acetylene 4

Chapter III

The $\tilde{X}$ AlOH - $\tilde{X}$ HAlO isomerization potential energy hypersurface 40

Chapter IV

Oxirene: To be or not to be? 63

Chapter V

Concluding Remarks 87

Chapter I: Introduction

I remember one beautiful spring day I was sitting in my undergraduate Quantum Mechanics and Atomic Physics class wishing that somehow we could hold class outside. Of course that would have been impossible because this particular physics professor always used the blackboard to derive everything from first principles. We'd solved Schrödinger's equation for the hydrogen atom about a month earlier, and all the lectures and homework problems since had been working toward solutions to multi-electron and multi-nuclear equations (where multi is generally taken to mean two). Even taking advantage of some minor approximations that the professor would allow us, these were long involved derivations filling reams of notebook paper and countless blackboards with equations. Perhaps, on this particular day, the weather was getting to him as well, because with at least five minutes left in the class period he stepped back from the board and said "Well, you can see where this is going, and that it is possible to solve this case if you're willing to work for it. But you can also see the situation gets complex rather quickly. What really impresses me is that the guys across the street (in the chemistry building) can solve this for several atoms and dozens of electrons. Don't ask me how though. It's left as an exercise for the inspired student to go ask them."

Well, I didn't walk across the street and ask. Instead I called up my friend, Brad DeLeeuw, who was then a first year graduate student in Quantum Chemistry. He did his best to explain everything to me over the phone, but what I got out of it was that Quantum Chemists took advantage of a couple more useful approximations and then used computers to do the bulk of the work. The thought of letting computers do the work for me had a nice ring to it, so to learn more I joined the summer undergraduate research program at the

Center for Computational Quantum Chemistry. In my naiveté I decided to have the computers solve the entire C_2H_2O potential energy hypersurface and determine, among other things, if oxirene was the symmetric stable intermediate in the Wolff decomposition of diazoketone to ketene. Over the course of the summer I barely had time to uncover the true difficulties of that surface and didn't have a real chance to solve any of them. And the problems of that surface have continually haunted me for most of my graduate career.

Dr. Yamaguchi tried to help me to reach some solutions in the oxirene problem during my first year of graduate school. He too decided that the problems of oxirene were too difficult, so he turned my attention to an easier set of species for which I might expect to successfully complete a project, the triplet acetylene and vinylidene surfaces. Along with ammonia and formaldehyde, acetylene is one of the three tetraatomic molecules most exhaustively characterized by spectroscopic techniques. Interestingly, though, many important energetic and spectral concerns for the low lying excited states of acetylene and their vinylidene isomers were not yet determined in the laboratory. So we undertook a study to provide as much theoretical insight as possible into that area of chemistry. The results of that research are presented in Chapter II.

During my second year of graduate school, another graduate student, Jeff Pilgrim, approached me with a question. In a study of aluminum and water clusters, he and Professor Duncan had uncovered an unexpected spectrum at 44 amu. Undoubtedly it was either HAlO or AlOH, but which? There wasn't enough available data in any journal articles for them to form a decision. Jeff asked if it were possible for me to quick calculate what he needed to know. I assured him that I would and sent him on his way. I got him those results (though perhaps not as quickly as he envisioned) and they are presented here in Chapter III.

With those research projects successfully under my belt, I returned my focus to the evils of the question about oxirene participation in the ketene rearrangement. Although I did wish to see the logic of science triumph over the complexities of nature, my real

motives for returning to this problem were not completely altruistic. Rather, everyone who knew I had started the oxirene project (not the least of whom was Professor Schaefer) wanted to know the results. The worst aspect of the study of the entire ketene - oxirene isomerization is that different levels of quantum chemical theory give different results. Some structures that are stationary points on the potential energy hypersurface at one level of theory disappear at other levels of theory. The oxirene stationary point itself switches from an equilibrium to a transition state with changes in the level of theory. Determination of which level of theory gives the correct qualitative results was a major problem. Presented in Chapter IV is my study of the oxirene potential energy surface to decide the best level of theory at which to study the entire isomerization reaction surface.

Chapter II

Isomerization Reactions on the Lowest Potential Energy Hypersurface of Triplet Vinylidene and Triplet Acetylene[1]

---

[1] G. V. Vacek, J. R. Thomas, B. J. DeLeeuw, Y. Yamaguchi and H. F. Schaefer *J. Chem. Phys.* **98**, 4766 (1993).

Triplet vinylidene, first predicted to have a sizable barrier to unimolecular rearrangement in 1978 by theory, has now been observed under three different sets of experimental conditions. In order to quantitatively characterize the potential energy hypersurface of triplet vinylidene and triplet acetylene, high-level *ab initio* quantum mechanical methods have been employed. Basis sets as large as triple zeta plus two sets of polarization functions augmented with higher angular momentum functions [TZ(2df,2pd)] have been utilized in conjunction with correlated methods as sophisticated as the coupled cluster approach including all single, double and perturbative triple excitations [CCSD(T)]. Of particular interest are predictions of the zero-point vibrational energy corrected barriers for rearrangement of $\tilde{a}\ ^3B_2$ vinylidene to $\tilde{b}\ ^3B_u$ *trans*-bent acetylene and of *cis*-bent $\tilde{a}\ ^3B_2$ acetylene to *trans*-bent $\tilde{b}\ ^3B_u$ acetylene. At the highest level of theory used here, TZ(2df,2pd) CCSD(T), these are predicted to be 47.9 kcal/mole and 13.0 kcal/mole, respectively. The physical properties of $\tilde{a}\ ^3B_2$ vinylidene, including the dipole moment, harmonic vibrational frequencies and the infrared intensities, have also been reported.

Introduction

For nearly a decade it was unclear whether singlet vinylidene

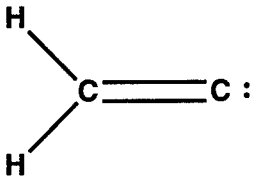

(1)

was a shallow minimum[1-3] on the C_2H_2 ground state potential energy hypersurface or merely a transition state[4,5] for the degenerate rearrangement of hydrogen atoms, e.g.

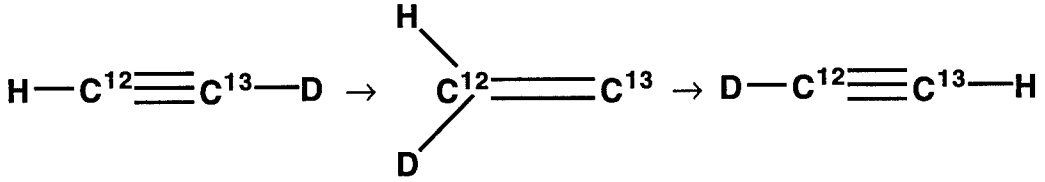

(2).

Recent negative ion photoelectron spectroscopy experiments by Ervin, Ho and Lineberger[6] have shown that the vinylidene potential well must be at least as deep as the experimentally observed $2\leftarrow0$ CH_2 rock transition, namely 450 cm^{-1} or 1.3 kcal/mole. The most recent

and extensive theoretical study by Gallo, Hamilton, and Schaefer[7] predicted a barrier of 1.6 kcal/mole including corrections for zero-point vibrational energies (ZPVE's).

In the case of triplet states of vinylidene, the situation is still somewhat nebulous. The first solid evidence that the $\tilde{a}\ ^3B_2$ state of vinylidene might be experimentally observable was provided by theory. In 1978, Conrad and Schaefer[8] predicted a classical barrier of 56 kcal/mole for its isomerization to the appropriate triplet state of acetylene using a basis set and method for the treatment of electron correlation effects that are of moderate quality by current standards. They also estimated the activation energy (including ZPVE corrections) to be about 50 kcal/mole. Shortly thereafter in flash photolysis experiments, Laufer[9] identified a reactive intermediate with composition C_2H_2 as the $\tilde{a}\ ^3B_2$ state of vinylidene. Laufer and coworkers[10] subsequently characterized the reactivity and quenching rates of this triplet state of vinylidene. In related work, Sülzle and Schwarz[11] observed a triplet state of vinylidene with a lifetime greater than 0.4 μsec by neutralization-reionization mass spectrometry.

The most quantitative energetic information concerning triplet vinylidene was provided by the negative ion photoelectron spectroscopy studies of Lineberger and coworkers.[6,12] They determined[6] singlet-triplet splittings of $T_0(\tilde{a}\ ^3B_2) = 47.6 \pm 0.1$ kcal/mole and $T_0(\tilde{b}\ ^3A_2) = 63.5 \pm 0.5$ kcal/mole for the two lowest excited states of vinylidene. Thus their experimentally observed value of $\Delta T_0(\tilde{b}\ ^3A_2 - \tilde{a}\ ^3B_2) = 15.9 \pm 0.6$ kcal/mole was obtained, in reasonable agreement with the earlier theoretical predictions of $\Delta T_e(\tilde{b}\ ^3A_2 - \tilde{a}\ ^3B_2) = 15.2$ kcal/mole by Dykstra and Schaefer[1] and $\Delta T_0(\tilde{b}\ ^3A_2 - \tilde{a}\ ^3B_2) =$ 13.9 kcal/mole by Osamura and Schaefer.[13] The very earliest prediction of the $^3B_2 - {}^3A_2$ energy separation by Davis, Goddard and Harding[14] was 26.6 kcal/mole.

In 1981 an interesting qualitative molecular orbital discussion of triplet vinylidene was presented by Harding[15] in the context of his excellent study of the vinyl and ethyl radicals and triplet methylcarbene. Noting that the doubly-occupied $5a_1$ lone pair orbital and an unoccupied p-π orbital in the $\tilde{b}\ ^3A_2$ state of vinylidene have characteristics which

strongly resemble the doubly-occupied $3a_1$ orbital and nonbonding *p*-type orbital in singlet methylene, he concluded that the $\tilde{b}\ ^3A_2$ state "should possess a low barrier to hydrogen migration analogous to that of other singlet carbenes." Harding also claimed that the transition state for isomerization to acetylene on the $^3A_2$ surface should be highly nonplanar. This leads to an avoided crossing of the $^3B_2$ and $^3A_2$ potential energy surfaces (PES's) at the C_1-symmetry transition state for 1,2-hydrogen shift.

Interaction between theory and experiment provided abundant evidence for the existence of low-lying triplet excited electronic states of acetylene. For example, theoretical prediction[16] followed quickly by experimental confirmation[17] left little doubt that a *cis*-bent $^3B_2$ state is the lowest excited state of acetylene. Nevertheless, Dupre, Jost, Lombardi, Green, Abramson and Field[18] have written the *only* experimental paper addressing these triplet states during the past three years. Surprisingly, the singlet-triplet splitting $T_0(\tilde{a}\ ^3B_2)$ has not yet been determined experimentally for acetylene. In addition, no experimentally observed spectroscopic features have been assigned to other low-lying electronic states, such as the predicted[16] *trans*-bent $\tilde{b}\ ^3B_u$ state. Theoretical work by Lischka and Karpfen[19] in 1986 and, more recently, by Yamaguchi, Vacek, and Schaefer[20] constitute the only high-level studies concentrating on these states since the ground-breaking 1978 theoretical study.[16] Both of these later works have focused on the molecular properties of stable minima on the triplet acetylene PES.

Based upon a recent analysis of Zeeman anticrossing (ZAC) spectra of gas phase acetylene,[18] it has been hypothesized that the S_1 excited singlet state of acetylene must lie close in energy to at least one of the isomerization transition states on the triplet PES of acetylene. Energetically speaking, the two most likely candidates are the transition state for *cis*-bent $\tilde{a}\ ^3B_2$ to *trans*-bent $\tilde{b}\ ^3B_u$ acetylene isomerization and the transition state for 1,2-hydrogen migration between $\tilde{a}\ ^3B_2$ vinylidene and $\tilde{b}\ ^3B_u$ acetylene. Information gained from a high-level theoretical study of these two transition states and the $\tilde{a}\ ^3B_2$ state of

vinylidene should prove quite useful in further experimental work on excited states of acetylene.

In light of the large body of experimental results,[6,9] it is remarkable that the 1978 work by Conrad and Schaefer[8] is the only theoretical study of 1,2-hydrogen migration in triplet vinylidene. Although theory assisted Laufer's 1980 discovery[9] of $\tilde{a}\ ^3B_2$ vinylidene, it is apparent that experiment has now taken a clear lead. Here we attempt to bring theory back as a synergetic partner. Ervin *et al.*[6] have observed three (out of six possible) fundamental vibrational frequencies for $\tilde{a}\ ^3B_2$ vinylidene. All six harmonic vibrational frequencies are reliably predicted here. Finally, quantitative predictions of the activation energy for 1,2-hydrogen migration in $\tilde{a}\ ^3B_2$ vinylidene and the related barrier for *cis-trans* triplet acetylene interconversion are made.

Electronic Structure Considerations

Ground state vinylidene is described in C_{2v} symmetry by the electronic configuration

$$[\text{core}](3a_1)^2(4a_1)^2(1b_2)^2(5a_1)^2(1b_1)^2 \qquad \tilde{X}\ ^1A_1 \text{ vinylidene} \qquad (3).$$

Note that [core] abbreviates the two lower-lying C 1s-like orbitals. The CC double bond in this structure consists of the $3a_1$ σ-bonding (σ^b) and the $1b_1$ π-bonding (π^b) orbitals. The highest occupied molecular orbital (HOMO) is the $1b_1$ π^b orbital. The $5a_1$ lone pair on the terminal (carbene) carbon is the second-highest occupied molecular orbital (SHOMO). These two HOMOs are energetically very close. The lowest unoccupied molecular orbital (LUMO), the $2b_2$ orbital, is essentially an in-plane nonbonding *p*-type orbital centered upon the terminal carbon. In this particular case, the electronic configuration of the lowest excited state of vinylidene, the $\tilde{a}\ ^3B_2$ state, differs from that of ground state vinylidene by excitation of a single electron from the SHOMO to the LUMO. Interestingly, exciting an electron from the HOMO to the LUMO of $\tilde{X}\ ^1A_1$ vinylidene leads to the second-lowest $\tilde{b}\ ^3A_2$ excited state of vinylidene. The reasons for this unusual ordering have been

discussed adequately by Dykstra and Schaefer.[1] Written in terms of C_{2v}-symmetry orbitals the electronic configurations of these two states are thus:

$$[\text{core}](3a_1)^2(4a_1)^2(1b_2)^2(1b_1)^2(5a_1)(2b_2) \qquad \tilde{a}\,^3B_2 \qquad (4);$$

$$[\text{core}](3a_1)^2(4a_1)^2(1b_2)^2(5a_1)^2(1b_1)(2b_2) \qquad \tilde{b}\,^3A_2 \qquad (5).$$

Based upon the electronic configuration (4) given above, the $\tilde{a}\,^3B_2$ state is expected to have a genuine CC double bond since both the $3a_1$ and $1b_1$ orbitals remain doubly-occupied. Because of the singly-occupied π^b orbital in its electron configuration (5), the $\tilde{b}\,^3A_2$ state is best considered to have a bond order of one and a half.

In its linear ground state, acetylene can be described by the electronic configuration

$$[\text{core}](2\sigma_g)^2(2\sigma_u)^2(3\sigma_g)^2(1\pi_u)^4 \qquad \tilde{X}\,^1\Sigma_g^+ \text{ acetylene} \qquad (6).$$

The $1\pi_u$ HOMO of this ground state is a π^b orbital, and the $1\pi_g$ LUMO is an antibonding (π^*) orbital. When acetylene is distorted to C_{2v} symmetry, the degenerate $1\pi_u$ HOMO splits into a lower-energy $1b_1$ orbital and a higher-energy $4a_1$ orbital, while the $1\pi_g$ LUMO becomes the $3b_2$ and $1a_2$ orbitals (with the $3b_2$ lower in energy). Thus, written in terms of C_{2v}-symmetry orbitals, the electronic configuration of ground state acetylene is

$$[\text{core}](2a_1)^2(2b_2)^2(3a_1)^2(1b_1)^2(4a_1)^2 \qquad (7).$$

The lowest excited triplet state has a *cis*-bent structure and belongs to the C_{2v} point group. Its electronic configuration is derived from (7) by excitation of a single electron from the HOMO to the LUMO:

$$[\text{core}](2a_1)^2(2b_2)^2(3a_1)^2(1b_1)^2(4a_1)(3b_2) \qquad \tilde{a}\,^3B_2 \qquad (8).$$

Distortion of linear ground state acetylene to *trans*-bent C_{2h} symmetry will cause a different splitting of the degenerate orbitals, namely $\pi^b \rightarrow 1a_u,3b_u$ and $\pi^* \rightarrow 4a_g,1b_g$. Written in terms of C_{2h}-symmetry MO's, the electronic configuration becomes

$$[\text{core}](2a_g)^2(2b_u)^2(3a_g)^2(1a_u)^2(3b_u)^2 \qquad (9)$$

for the ground state of acetylene. Excitation of an electron from the $3b_u$ HOMO to the $4a_g$ LUMO results in the second-lowest triplet state of acetylene. This triplet state has a *trans*-bent structure with the electronic configuration

$$[\text{core}](2a_g)^2(2b_u)^2(3a_g)^2(1a_u)^2(3b_u)(4a_g) \qquad \tilde{b}\ ^3B_u \qquad (10).$$

The $\tilde{X}\ ^1\Sigma_g^+$ state of acetylene has a prototypical triple bond (one σ bond and two π bonds). In both excited states of acetylene discussed above, the carbon-carbon bond involves two electrons in the σ^b orbital, three in π^b orbitals, and one in a π^* orbital. Therefore, the $\tilde{a}\ ^3B_2$ and $\tilde{b}\ ^3B_u$ states of acetylene are expected to exhibit double-bond characteristics.

Under the constraint of C_s symmetry with the σ_h symmetry element defined by the molecular plane, the qualitative electronic configurations of $\tilde{a}\ ^3B_2$ vinylidene, $\tilde{a}\ ^3B_2$ acetylene and $\tilde{b}\ ^3B_u$ acetylene may all be written as

$$[\text{core}](3a')^2(4a')^2(5a')^2(1a'')^2(6a')(7a') \qquad ^3A' \qquad (11).$$

Though they may have identical *qualitative* electronic configurations, each MO may have a significantly different nature in each of these three triplet states. Incidentally, the qualitative electronic configuration of any planar transition state between these three triplet states on the C_2H_2 triplet surface is also represented by (11). On the other hand, written in terms of C_s-symmetry MO's with the molecular plane again defining σ_h, the $\tilde{b}\ ^3A_2$ state of vinylidene has the electronic configuration

$$[\text{core}](3a')^2(4a')^2(5a')^2(6a')^2(1a'')(7a') \qquad ^3A'' \qquad (12).$$

Distortion of the molecular electronic states described by equations (11) and (12) into C_1 symmetry changes the qualitative electronic configurations to

$$[\text{core}](3a)^2(4a)^2(5a)^2(6a)^2(7a)(8a) \qquad ^3A \qquad (13).$$

Thus all the triplet states of C_2H_2 mentioned above become indistinct when distorted into C_1 symmetry.

Theoretical Procedures

Three basis sets were employed in this study. The first basis set was of double-zeta plus polarization (DZP) quality. It consisted of a standard Huzinaga-Dunning double-zeta set[21,22] of contracted Gaussian functions [designated (9s5p/4s2p) for carbon and (4s/2s) for hydrogen] augmented with a single set of d-like polarization functions on C and p

functions on H. The exponents of the polarization functions were $\alpha_d(C) = 0.75$ and $\alpha_p(H) = 0.75$. The triple-zeta plus two sets of polarization functions (TZ2P) basis set was composed of Dunning's[23] (5s3p) contraction of Huzinaga's[21] (10s6p) primitive set of Gaussian functions for carbon and Dunning's[23] (3s) contraction of Huzinaga's[21] (5s) set for hydrogen augmented with two sets of polarization functions for each atom. The polarization function orbital exponents were $\alpha_d(C) = 1.50$, 0.375 and $\alpha_p(H) = 1.50$, 0.375. The final basis set was formed by supplementing the TZ2P basis with higher angular momentum polarization functions [$\alpha_f(C) = 0.8$ and $\alpha_d(H) = 1.0$]. This basis set has been designated TZ(2df,2pd). Throughout this study, sets of six Cartesian d-like and ten Cartesian f-like polarization functions were employed.

The molecular structures of the lowest triplet state of vinylidene and the transition states for isomerization reactions were fully optimized using analytic gradient techniques for restricted Hartree-Fock self-consistent field (SCF)[24,25] and configuration interaction (CI) wavefunctions.[26,27] In all cases, the residual Cartesian and internal coordinate gradients were less than 10^{-6} atomic units. Analytic second derivative procedures[28,29] were used to evaluate the quadratic force constants for the SCF wavefunctions.

CI and coupled cluster (CC) methods were employed to include the effects of electron correlation. All single and double excitations from the SCF reference configuration were included (CISD and CCSD), with the exception that only the valence electrons were explicitly correlated. In this manner, the two lowest-lying MOs (C 1s-like) were held doubly-occupied (frozen cores), and the two highest-lying orbitals (C 1s*-like) were excluded (deleted virtuals) from the configuration space. With the TZ(2df,2pd) basis set, this correlation scheme involved 38,585 configurations for the C_{2v}-symmetry wavefunction of $^3B_2$ vinylidene, 144,777 configurations for the C_1-symmetry transition state from $^3B_2$ vinylidene to ^3B_u acetylene, and 76,557 configurations for the C_s-symmetry transition state to interconversion between $^3B_2$ acetylene and ^3B_u acetylene in the Hartree-Fock interacting space[30,31] for the CISD and CCSD wavefunctions. The shape driven

graphical unitary group approach[32] was used to obtain CISD wavefunctions. An estimate of the contribution of unlinked-cluster-quadruple-excitations to the CISD energies was obtained via Davidson's correction.[33,34] Such results are designated CISD+Q. The method of finite central differences of analytic gradients[26,27] was utilized to evaluate the quadratic force constants for the CISD wavefunctions.

Open-shell CCSD wavefunctions were constructed using the methodology developed by Scuseria.[35] This follows an approach originally developed by Purvis and Bartlett[36] for the closed-shell case and modified by Scuseria and Janssen.[37] The effect of connected triple excitations was included using the perturbative approach suggested by Raghavachari, Trucks, Pople and Head-Gordon [CCSD(T)][38] and implemented in our group by Scuseria.[35] Improved predictions of relative energies with a particular basis set were obtained by evaluating coupled cluster single-point energies at the corresponding CISD optimized geometries. The textual notation used to designate such single-point energy calculations in this paper is as follows: a DZP CCSD(T) single-point energy evaluated at the DZP CISD optimized geometry will be referred to as DZP CCSD(T)//CISD.

Results

Equilibrium structures predicted for $\tilde{a}\ ^3B_2$ vinylidene are presented in Figure 1. The optimized geometries for the two "true" transition state structures (i.e. those having only one imaginary frequency) are shown in Figures 2, 3 and 4. Two other stationary points that were examined on the DZP SCF surface and found to have *more* than one imaginary frequency are discussed below but not depicted.

The harmonic vibrational frequencies predicted for the three stationary points, as well as the total energies, dipole moments and ZPVEs are listed in Tables I, III and IV. The corresponding infrared (IR) intensities for $\tilde{a}\ ^3B_2$ vinylidene are also given in Table I. Harmonic vibrational frequencies for isotopically substituted $\tilde{a}\ ^3B_2$ d_1- and d_2-vinylidenes

are presented in Table II. It should be noted that the vibrational frequencies predicted by this research are *harmonic* frequencies in all cases, not fundamentals; thus the contribution of anharmonic terms is not included in our results.

The CISD+Q, CCSD, and CCSD(T) total energies determined at CISD optimized geometries are shown in Table V. Relative energies of $\tilde{a}\ ^3B_2$ vinylidene with respect to $\tilde{X}\ ^1A_1$ vinylidene given in Table VI were obtained using energetic information from Tables I and V as well as results published by Gallo *et al.*[7] where possible. Relative energies of the other studied stationary points with respect to $\tilde{a}\ ^3B_2$ acetylene are summarized in Table VII and have been obtained using the energetic information presented in Tables I, and III - V. Relative energies of the $\tilde{b}\ ^3B_u$ state of acetylene were also included in Table VII to allow more detailed comparison. The values used for these two triplet states of acetylene are taken directly from our previous study[20] for identical basis sets and methods. For the CISD+Q, CCSD and CCSD(T) energies, the CISD ZPVE values for the corresponding basis sets were employed to make best-estimate corrections.

In some cases, no previously reported information was available for $\tilde{X}\ ^1A_1$ vinylidene, $\tilde{a}\ ^3B_2$ acetylene and $\tilde{b}\ ^3B_u$ acetylene at levels of theory consistent with this work. For these states, previously unreported harmonic vibrational frequencies and energetic data determined in this research are presented in Appendix A. None of these results were qualitatively different from those reported in earlier works[7,20] for the relevant states.

Discussion

Geometries

$\tilde{a}\ ^3B_2$ Vinylidene

Based upon the results of their Franck-Condon simulations of observed spectra, Ervin *et al.*[6] reported an "experimentally determined" molecular geometry for $\tilde{a}\ ^3B_2$ vinylidene: $r_e(CC) = 1.346 \pm 0.040$ Å, $r_e(CH) = 1.090 \pm 0.009$ Å, and $\theta_e(HCH) = 118.9$

$\pm 2.7°$. The Franck-Condon simulations were optimized relative to the molecular structure of $\tilde{X}\ ^1A_1$ vinylidene predicted[3] at the TZ + P CISD level of theory. Therefore, it is not very surprising that all of the CISD geometric parameters for the $\tilde{a}\ ^3B_2$ state of vinylidene shown in Figure 1 fall safely within the experimentally reported error margins.

A comparison of the $\tilde{a}\ ^3B_2$ vinylidene geometry in Figure 1 with that of $\tilde{X}\ ^1A_1$ vinylidene reported by Gallo *et al.*[7] at comparable levels of theory reveals the small changes in geometry that result from exciting an electron from the $5a_1$ *sp*-type lone pair MO to the $2b_2$ nonbonding *p*-type MO. The CC bond slightly elongates in $\tilde{a}\ ^3B_2$ vinylidene [r_e(CC) = 1.3121 Å at TZ2P CISD] relative to the ground state [r_e(CC) = 1.2957 Å at TZ2P CISD],[7] but both states obviously involve CC double bonds. (In ethylene, the experimental double-bond length is r_0(CC) = 1.337 Å).[39] The HCH angle is 2° smaller in the $\tilde{a}\ ^3B_2$ state than in the $\tilde{X}\ ^1A_1$ state due to interaction between the singly-occupied $2b_2$ orbital and the $1b_2$ CH orbital. There is no significant change in the CH bond lengths between the $\tilde{a}\ ^3B_2$ and $\tilde{X}\ ^1A_1$ states of vinylidene.

Transition State for Triplet Vinylidene ↔ Triplet Acetylene Isomerization

An initial search was made for a planar transition state for the $^3B_2$ vinylidene ↔ ^3B_u acetylene isomerization reaction. A stationary point with a "bridged" structure similar to that previously reported by Conrad *et al.*[8] was readily found. At the DZP SCF level, the optimized geometry is $r_e(C_1C_2)$ = 1.291Å, $r_e(C_1H_{bridged})$ = 1.250Å, $r_e(C_2H_{nonbridged})$ = 1.089Å, $\theta_e(C_2C_1H_{bridged})$ = 60.5°, $\theta_e(C_1C_2H_{nonbridged})$ = 135.3°. Vibrational analysis of this structure, however, revealed a $2780i$ cm^{-1} a' imaginary mode corresponding to in-plane motion of the migrating (bridging) hydrogen and a $735i$ cm^{-1} a" imaginary mode corresponding to an HCCH torsional motion. This C_s-symmetry structure is thus properly characterized as a higher-order saddle point with a Hessian index of two. The true isomerization transition state with a Hessian index of one should therefore belong to the C_1-symmetry point group.

When the C_s-symmetry constraint was removed, the genuine C_1-symmetry isomerization transition state was located. Its structure is shown in Figure 2. The CC bond length predicted for this structure (e.g. 1.410Å for TZ2P CISD) implies that the transition state structure involves a bond of order one and a half between the carbon atoms. This is distinctly different from the doubly-bonded [r_e(CC) = 1.244Å at TZ2P CISD][7] C_s-symmetry transition state structure predicted for isomerization of $\tilde{X}\ ^1A_1$ vinylidene to $\tilde{X}\ ^1\Sigma_g^+$ acetylene. Another notable difference between the C_2H_2 singlet ground-state PES and this excited triplet state PES is that the transition state structure for 1,2-hydrogen migration in the former is planar[7] while it is nonplanar in the latter. In fact, the torsional angle between the HCC planes for the latter (depicted in Figure 3) is 115.7° at the TZ(2df,2pd) CISD level of theory. Thus, in the case of the 1,2-hydrogen shift transition state for $\tilde{a}\ ^3B_2$ vinylidene, the migrating hydrogen lies in a position nearly perpendicular to the plane of the other three atoms rather than lying in that plane.

The geometrical differences between the isomerization transition state structures on the singlet ground-state PES and the triplet excited-state PES can be attributed to two effects. First, in the nonplanar triplet isomerization transition state, the CC π bond breaks and the methylene carbon hybridization changes as the CHC two-electron-three-center bond forms during 1,2 hydrogen migration. Second, as Harding stated so succinctly,[15] there is an avoided crossing of the two lowest triplet state PES's in C_1-symmetry. The 1,2-hydrogen shift transition state for $\tilde{b}\ ^3A_2$ vinylidene should have a long CC single bond and an overall structure that is strongly nonplanar. The mixing of these two states produces an isomerization transition state for the lowest triplet state with a longer CC bond distance and a nonplanar structure. For the lowest triplet state surface, this mixing also significantly lowers the activation barrier to hydrogen migration via a C_1-symmetry path relative to that of the C_s-symmetry reaction pathway.

Transition State for cis-trans Triplet Acetylene Isomerization

Initial searches for the isomerization transition state between $\tilde{b}\ ^3B_u$ and $\tilde{a}\ ^3B_2$ acetylene were performed along two paths of inquiry. The first *cis-trans* isomerization transition state was sought under C_2-symmetry constraints with interconversion taking place through rotation about the CC axis. Another possible isomerization path was an in-plane inversion. The second search was therefore made under the constraint of C_s-symmetry.

The search for a C_2-symmetry transitions state at the DZP SCF level led to a structure with linear geometry: $r_e(CC) = 1.327$Å and $r_e(CH) = 1.058$Å. Vibrational analysis revealed that this structure has a Hessian index of two, indicating that it is a higher-order saddlepoint and *not* a true transition state. The first imaginary frequency, a *trans*-bending a-symmetry mode, had a magnitude of $1379i$ cm^{-1}. The second imaginary frequency, $1550i$ cm^{-1}, corresponds to a *cis*-bending b-symmetry mode.

The true triplet *cis-trans* isomerization transition state, illustrated in Figure 4, was found to have C_s symmetry. The geometry of this structure is about what one would expect for an inversion isomerization reaction. The inverting hydrogen is very nearly collinear with the CC bond axis, but it is 4-6° *trans*-bent with respect to the other hydrogen. This structure agrees with Hammond's Postulate[40] since the *cis*-bent $^3B_2 \rightarrow$ *trans*-bent ^3B_u acetylene interconversion is an endothermic reaction. The bond lengths and angles are reasonably close to the related geometrical parameters of both the *cis*- and *trans*-bent minima,[20] with the exception of the CH bond length of the inverting hydrogen. In the $\tilde{a}\ ^3B_2$ and $\tilde{b}\ ^3B_u$ triplet states of acetylene, the orbitals of the carbon atoms in the CH bonds may be thought of as typical sp^2-hybridized orbitals. In the inversion transition state structure, however, the orbital of the carbon atom in the $CH_{inverting}$ bond is best viewed as an *sp*-hybrid orbital. The greater *s*-character leads to the shorter $CH_{inverting}$ bond length relative to the other CH bond length.

Harmonic Vibrational Frequencies

$\tilde{a}\,^3B_2$ Vinylidene

The three experimentally observed a_1 fundamental frequencies reported by Ervin *et al.*[6] [CH symmetric stretch 2930 ± 10 cm^{-1}, CC stretch 1530 ± 70 cm^{-1} and CH_2 scissors 1375 ± 10 cm^{-1}] agree well with the corresponding harmonic frequencies listed in Table I. For example, at the TZ(2df,2pd) CISD level of theory we have predicted the harmonic frequencies for the corresponding a_1 modes to be 3143 cm^{-1}, 1637 cm^{-1} and 1451 cm^{-1}. If a harmonic-to-fundamental scaling factor is employed (typically 0.92 - 0.96 at levels including electron correlation),[41-45] the agreement becomes remarkably good. In the case of $\tilde{a}\,^3B_2$ C_2D_2 (see Table II), Ervin *et al.*[6] reported fundamental frequencies of 2160 ± 10 cm^{-1}, 1495 ± 10 cm^{-1} and 1010 ± 10 cm^{-1} for the CD symmetric stretch, the CC stretch and CD_2 scissors modes, respectively. At the TZ(2df,2pd) CISD level of theory, we predict them (unscaled) to be 2284 cm^{-1}, 1604 cm^{-1} and 1058 cm^{-1}. Experimentally observed isotopic shifts (C_2H_2 - C_2D_2) are 770 (2930-2160) cm^{-1}, 35 (1530-1495) cm^{-1} and 365 (1375-1010) cm^{-1}, respectively, while theoretically predicted (harmonic) isotopic shifts are 859 (3143-2284) cm^{-1}, 33 (1637-1604) cm^{-1} and 393 (1451-1058) cm^{-1}. The agreement between experimental and theoretical isotopic shifts is very satisfactory and consistently good at all levels of theory utilized in this paper.

Transition State for Triplet Vinylidene ↔ Triplet Acetylene Isomerization

The C_1-symmetry transition state for isomerization between $\tilde{a}\,^3B_2$ vinylidene and $\tilde{b}\,^3B_u$ *trans*-bent acetylene has been confirmed by vibrational analysis to be a true transition state with a Hessian index of one at all levels of theory employed in this work (see Table III). According to a potential energy distribution (PED) analysis of the normal mode with one imaginary frequency, the reaction coordinate consists of the $CCH_{migrating}$ bend and the $CH_{migrating}$ stretch. With the TZ(2df,2pd) basis, the imaginary frequency was determined to be 1731*i* cm^{-1} by the SCF method and 1500*i* cm^{-1} by the CISD method. At the same

levels of theory, the lowest real harmonic vibrational frequency was determined to be 836 cm^{-1} and 777 cm^{-1}, respectively. The large magnitudes of the imaginary frequency and the lowest real harmonic vibrational frequency suggest that the nature of this stationary point will not change even if more sophisticated correlated methods are employed.

The harmonic vibrational frequency for the CC stretch is 1637 cm^{-1} for $\tilde{a}\ ^3B_2$ vinylidene and 1640 cm^{-1} for $\tilde{b}\ ^3B_u$ acetylene at the TZ(2df,2pd) CISD level of theory; the CC stretch mode for the transition state connecting these two minima has a frequency of only 1355 cm^{-1}. This red-shift of about 285 cm^{-1} is due to the lengthening of the CC bond in the transition state (bond order one and a half) relative to the doubly-bonded minima. Not surprisingly, the vibrational frequency associated with the $CH_{migrating}$ stretching mode is also greatly decreased in the transition state structure due to the ~0.1Å increase of that bond length. The average of the two TZ(2df,2pd) CISD CH stretching frequencies of $\tilde{a}\ ^3B_2$ vinylidene is 3190 cm^{-1}, and for $\tilde{b}\ ^3B_u$ acetylene the corresponding average is 3256 cm^{-1}. In the transition state structure, however, the harmonic vibrational frequency for the $CH_{migrating}$ mode is 2316 cm^{-1}, which is red-shifted by ~900 cm^{-1}. These frequency shifts with changes in bond lengths are expected from Badger's Rules.[46]

Transition State for cis-trans Triplet Acetylene Isomerization

Vibrational analysis of this C_s-symmetry stationary point has confirmed the structure to be a genuine transition state with only one imaginary vibrational frequency at all levels of theory (see Table IV). The reaction coordinate is mainly the $CCH_{inverting}$ bend. In contrast with the transition state discussed in the previous section, there is almost no $CH_{inverting}$ stretch contribution to the reaction coordinate. The magnitude of the imaginary vibrational frequency is very stable with respect to basis set improvements, and it only decreases by about 150 cm^{-1} for CISD results relative to SCF results. For example, with the TZ(2df,2pd) basis set, SCF theory predicts a magnitude of 1147*i* cm^{-1}, while the CISD method predicts 995*i* cm^{-1}. The stability of this imaginary frequency and the lowest

real vibrational frequency, the a" out-of-plane bending mode, strongly suggest that the nature of this stationary point will not change even with more sophisticated *ab initio* methods.

As previously mentioned, this transition state structure has a CC double bond. It is expected to have a CC stretch vibrational frequency similar to those of $\tilde{a}\ ^3B_2$ and $\tilde{b}\ ^3B_u$ acetylene. In fact, the TZ(2df,2pd) CISD CC stretch frequency of 1633 cm^{-1} for this transition state structure is about the same as the CC stretch frequencies of 1660 cm^{-1} and 1640 cm^{-1} predicted for $\tilde{a}\ ^3B_2$ and $\tilde{b}\ ^3B_u$ acetylene with an equivalent level of theory.[20] Furthermore, the other real frequencies have magnitudes similar to the corresponding vibrational frequencies in the two lowest triplet states of acetylene.

Energetics

$\tilde{a}\ ^3B_2$ Vinylidene

In comparison with results published by Ervin *et al.*,[6] the *ab initio* theoretical predictions for the ($\tilde{X}\ ^1A_1$ - $\tilde{a}\ ^3B_2$) vinylidene energy separation are quite reasonable. At all correlated levels these results (see Table VII) fall within about 6 kcal/mole of the experimentally reported value. The theoretically predicted values approach the experimentally reported value from below in all cases as the basis set size is increased. Inclusion of electron correlation, also tends to increase the predicted singlet-triplet splittings. As improvements in the treatment of electron correlation are made using the same basis set, the predicted value of the splitting seems to converge toward a single value. This would seem to indicate that the CCSD(T) single-point energy evaluations at the CISD optimized geometries recover most of the electron correlation energy for both of these states of vinylidene. Our results at the TZ(2df,2pd) CCSD(T)//CISD level of theory agree remarkably well with experimentally reported values. Specifically, our study obtains the result $T_e(\tilde{X}\ ^1A_1$ - $\tilde{a}\ ^3B_2)$ = 45.58 kcal/mole compared with the experimental value[6] of 46.8 ± 0.5 kcal/mole. Likewise, our theoretical prediction of $T_0(\tilde{X}\ ^1A_1$ - $\tilde{a}\ ^3B_2)$ at that level of

theory is 46.56 kcal/mole, while the experimentally reported value[6] is 47.60 ± 0.14 kcal/mole. Experimental and theoretical agreement to within 1 kcal/mole is generally considered excellent. This instills confidence that all of our energetic predictions at the TZ(2df,2pd) CCSD(T)//CISD level of theory should be within 1.5 kcal/mole of the true values.

As shown in the last column of Table VI, the "triplet-triplet" splitting between $\tilde{a}\ ^3B_2$ vinylidene and $\tilde{a}\ ^3B_2$ acetylene is in the neighborhood of 1–3 kcal/mole. The classical energy difference increases slightly with basis set improvements [e.g. 2.4 kcal/mole for DZP SCF to 2.6 for TZ(2df,2pd) SCF] and generally decreases by including electron correlation [e.g. 0.9 for DZP CCSD(T)//CISD]. The best value predicted in this work, with ZPVE corrections, is $\Delta E_0(\tilde{a}\ ^3B_2$ vinylidene - $\tilde{a}\ ^3B_2$ acetylene) = 2.2 kcal/mole for TZ(2df,2pd) CCSD(T)//CISD.

Triplet Vinylidene ↔ Triplet Acetylene Isomerization

The theoretically predicted energies for the two minima involved in this isomerization reaction, determinable from Table VI, differ by 5-6 kcal/mole. With ZPVE corrections, at the TZ(2df,2pd) CCSD(T)//CISD level of theory, this energy difference is 6.1 (8.3 - 2.2) kcal/mole. The reaction, although it is slightly endothermic, is thus nearly thermoneutral.

With the DZP basis, the classical barrier to isomerization via 1,2-hydrogen shift for the SCF method is 60.7 (63.1 - 2.4) kcal/mole, but it drops by almost 4 kcal/mole to 56.9 (58.4 - 1.5) kcal/mole for the CISD method and drops further to 53.2 (54.1 - 0.9) kcal/mole for the CCSD(T)//CISD method. Basis set improvements are generally accompanied by decreases in the predicted value of the classical barrier. For example, with the CCSD(T)//CISD method, improvement of the basis set quality from DZP to TZ(2df,2pd) leads to a drop in the classical barrier by over one kcal/mole to 52.1 (53.6 - 1.5) kcal/mole. Finally, for all basis sets, the ZPVE correction lowers the barrier

significantly. At the TZ(2df,2pd) CCSD(T)//CISD level of theory, with CISD ZPVE corrections, the barrier to isomerization via 1,2-hydrogen migration is 47.9 (50.1 - 2.2) kcal/mole. For the reverse reaction, the barrier is 41.8 (50.1 - 8.3) kcal/mole.

The barrier to isomerization predicted for the forward reaction is much higher than the analogous barrier for the ground state vinylidene reaction of 1.6 kcal/mole.[7] In the case of the singlet ground state, facile rearrangement (admittedly, with extensive rehybridization of the MO's) can take place by migration of the H atom toward the unoccupied in-plane *p*-type orbital on the carbene carbon. On the other hand, in the case of ã $^3B_2$ rearrangement, the *p*-type MO is singly-occupied. The resultant repulsive interactions make the in-plane migration an extremely high-energy pathway. This forces the triplet 1,2-hydrogen migration to take place via another pathway. At the DZP SCF level of theory, the C_s-symmetry-constrained higher-order saddle point lies 18.4 kcal/mole above the C_1-symmetry transition state.

Transition State for cis-trans Triplet Acetylene Isomerization

Based upon single-point energies evaluated using the CI method with a basis set slightly larger in size than our DZP, Demoulin[47] suggested that the classical barrier to *cis-trans* triplet acetylene interconversion by internal rotation about the CC bond is about 23.1 kcal/mole and 18.9 kcal/mole for the reverse reaction. As discussed in the geometry section above, a corresponding stationary point along the internal rotation coordinate was located at the DZP SCF level of theory with a total energy of -76.671923 hartrees. This places it 35.3 kcal/mole in energy above ã $^3B_2$ acetylene, although it is not a true transition state. By comparison, the classical barrier to interconversion along an inversion pathway is only 17.3 kcal/mole at the DZP SCF level of theory. Inversion is thus the energetically preferred process for the *cis-trans* isomerization.

As shown in the third column of Table VI, the barrier to *cis-trans* isomerization via in-plane inversion decreases with both basis set improvements and inclusion of electron

correlation effects. According to arguments similar to those presented in the previous two sections, the predicted barriers should converge to within a couple kcal/mole of the true value. At the TZ(2df,2pd) CCSD(T)//CISD level of theory, we found the ZPVE corrected barrier to be 13.0 kcal/mole.

The exothermic reverse reaction, *trans-cis* triplet acetylene interconversion by inversion, has a markedly lower barrier to rearrangement. Our best prediction of the *trans-cis* triplet acetylene isomerization barrier is 4.7 (13.0 - 8.3) kcal/mole with ZPVE corrections at the TZ(2df,2pd) CCSD(T)//CISD level of theory. Although this barrier is quite small, it is unlikely to disappear entirely at higher levels of theory.

Conclusion

High-level *ab initio* molecular electronic structure theory has been applied to investigate the $\tilde{a}\ ^3B_2$ electronic state of vinylidene, the transition state for isomerization of $\tilde{a}\ ^3B_2$ vinylidene to $\tilde{b}\ ^3B_u$ *trans*-bent acetylene, and the transition state for interconversion between $\tilde{a}\ ^3B_2$ *cis*-bent and $\tilde{b}\ ^3B_u$ *trans*-bent acetylene.

The $\tilde{a}\ ^3B_2$ state of vinylidene is confirmed to be a doubly-bonded minimum-energy structure at all levels of theory. Predicted harmonic vibrational frequencies agree well with available experimental fundamental frequencies for $\tilde{a}\ ^3B_2$ vinylidene and for the mono- and di- deuterated isotopomers of $\tilde{a}\ ^3B_2$ vinylidene. Theoretical predictions of $T_0(\tilde{X}\ ^1A_1 - \tilde{a}\ ^3B_2)$ for vinylidene are also in excellent agreement with the results of negative ion photoelectron spectroscopy experiments.

A nonplanar bridged structure was found to be the transition state for the rearrangement of $\tilde{a}\ ^3B_2$ vinylidene to $\tilde{b}\ ^3B_u$ *trans*-bent acetylene. The barrier to 1,2-hydrogen migration was found to be 47.9 kcal/mole at the highest level of theory, TZ(2df,2pd) CCSD(T)//CISD.

The unimolecular reaction which interconverts $\tilde{a}\ ^3B_2$ *cis*-bent and $\tilde{b}\ ^3B_u$ *trans*-bent acetylene was found to occur via a planar inversion pathway rather than by rotation about

the CC bond axis. The barrier for this inversion process was shown to be only 13.0 kcal/mole at the highest level of theory.

Acknowledgements

This research was supported by the U. S. Department of Energy, Office of Basic Energy Sciences, Division of Chemical Sciences, Fundamental Interactions Branch, Grant No. DE-FG09-87ER13811. The work done on this research was supported in part by DOD and NSF graduate fellowships. For his encouragement to initiate this study, the authors would like to thank Professor Robert W. Field at the Massachusetts Institute of Technology. We would like to thank Dr. Roger Grev for insightful comments, and Oh Soon, Dee Dee and Joann for support.

Appendix A

The TZ(2df,2pd) CISD harmonic vibrational frequencies for the $^3B_2$ state of acetylene are 3196 cm^{-1}, 1660 cm^{-1}, and 849 cm^{-1} for the a_1 modes. The a_2 mode frequency is 839 cm^{-1}, and the b_2 modes predictions are 3160 cm^{-1} and 1133 cm^{-1}. Those for the ^3B_u state of acetylene are 3265 cm^{-1}, 1640 cm^{-1}, and 1124 cm^{-1} for the a_g modes, 937 cm^{-1} for the a_u mode, and 3247 cm^{-1} and 791 cm^{-1} for the b_u modes.

For the DZP and TZ2P basis sets, the CCSD//CISD energies of $\tilde{X}\ ^1A_1$ vinylidene are -77.038632 and -77.078175, respectively. For CCSD(T)//CISD with those basis sets, the energies are -77.047967 and -77.090869. With the TZ(2df,2pd) basis set, the SCF energy at the optimized geometry is -76.795671. Harmonic vibrational frequencies at this level of theory are 3363 cm^{-1}, 3274 cm^{-1}, 1819 cm^{-1}, 1352 cm^{-1}, 912 cm^{-1} and 523 cm^{-1}. The TZ(2df,2pd) CISD energy is -77.081828 hartrees. Harmonic vibrational frequencies for this level of theory are 3294 cm^{-1}, 3201 cm^{-1}, 1732 cm^{-1}, 1265 cm^{-1}, 798 cm^{-1} and 376 cm^{-1}. The TZ(2df,2pd) CISD+Q//CISD, CCSD//CISD and CCSD(T)//CISD energies are -77.110428 hartrees, -77.105181 hartrees and -77.119439 hartrees, respectively.

References

1. C. E. Dykstra and H. F. Schaefer, *J. Am. Chem. Soc.* **100**, 1378 (1978).
2. Y. Osamura, H. F. Schaefer, S. K. Gray and W. H. Miller, *J. Am. Chem. Soc.* **103**, 1904 (1981).
3. T. Carrington, L. M. Hubbard, H. F. Schaefer and W. H. Miller, *J. Chem. Phys.* **80**, 4347 (1984).
4. R. Krishnan, M. J. Frisch, J. A. Pople and P. v. R. Schleyer, *Chem. Phys. Lett.* **79**, 408 (1981).
5. J. A. Pople, *Pure Appl. Chem.* **55**, 343 (1983).
6. K. M. Ervin, J. Ho and W. C. Lineberger, *J. Chem. Phys.* **91**, 5974 (1989).
7. M. M. Gallo, T. P. Hamilton and H. F. Schaefer, *J. Am. Chem. Soc.* **112**, 8714 (1990).
8. M. P. Conrad and H. F. Schaefer, *J. Am. Chem. Soc.* **100**, 7820 (1978).
9. A. H. Laufer, *J. Chem. Phys.* **73**, 49 (1980).
10. A. H. Laufer, *J. Chem. Phys.* **76**, 945 (1982); A. H. Laufer and Y. L. Yung, *J. Phys. Chem.* **87**, 181 (1983); A. H. Laufer, *Chem. Phys. Lett.* **94**, 240 (1983); *J. Photochem.* **27**, 267 (1984); A. Fahr and A. H. Laufer, *J. Chem. Phys.* **83**, 908 (1985); *J. Phys. Chem.* **89**, 2906 (1985); *ibid.* **90**, 5064 (1986); *J. Photochem.* **34**, 261, (1986); *J. Am. Chem. Soc.* **109**, 3843 (1987); A. Fahr and A. H. Laufer, *J. Phys. Chem.* **96**, 4217 (1992).
11. D. Sülzle and H. Schwarz, *Chem. Phys. Lett.* **156**, 397 (1989).
12. S. M. Burnett, A. E. Stevens, C. S. Feigerle and W. C. Lineberger, *Chem. Phys. Lett.* **100**, 124 (1983).
13. Y. Osamura and H. F. Schaefer, *Chem. Phys. Lett.* **79**, 412 (1981).
14. J. H. Davis, W. A. Goddard and L. B. Harding, *J. Am. Chem. Soc.* **99**, 2919 (1977).

15. L. B. Harding, *J. Am. Chem. Soc.* **103**, 7469 (1981).

16. R. W. Wetmore and H. F. Schaefer, *J. Chem. Phys.* **69**, 1648 (1978).

17. H. R. Wendt, H. Hippler and H. E. Hunziker, *J. Chem. Phys.* **70**, 4044 (1979).

18. P. Dupre, R. Jost, M. Lombardi, P. G. Green, E. Abramson and R. W. Field, *Chem. Phys.* **152**, 293 (1991).

19. H. Lischka and A. Karpfen, *Chem. Phys.* **77**, 102 (1986).

20. Y. Yamaguchi, G. Vacek and H. F. Schaefer, *Theor. Chim. Acta.* **86**, 97 (1993).

21. S. Huzinaga, *J. Chem. Phys.* **42**, 1293 (1965).

22. T. H. Dunning, *J. Chem. Phys.* **53**, 2823 (1970).

23. T. H. Dunning, *J. Chem. Phys.* **55**, 716 (1971).

24. J. D. Goddard, N. C. Handy and H. F. Schaefer, *J. Chem. Phys.* **71**, 1525 (1979).

25. Y. Osamura, Y. Yamaguchi and H. F. Schaefer, *J. Chem. Phys.* **77**, 383 (1982).

26. B. R. Brooks, W. D. Laidig, P. Saxe, J. D. Goddard, Y. Yamaguchi and H. F. Schaefer, *J. Chem. Phys.* **72**, 4652 (1980).

27. J. E. Rice, R. D. Amos, N. C. Handy, T. J. Lee and H. F. Schaefer, *J. Chem. Phys.* **85**, 963 (1986).

28. Y. Osamura, Y. Yamaguchi, P. Saxe, M. A. Vincent and H. F. Schaefer, *Chem. Phys.* **72**, 131 (1982).

29. Y. Yamaguchi, Y. Osamura, P. Saxe, D. J. Fox, M. A. Vincent and H. F. Schaefer, *J. Mol. Struct.* **103**, 183 (1983).

30. A. Bunge, *J. Chem. Phys.* **53**, 20 (1970).

31. C. F. Bender and H. F. Schaefer, *J. Chem. Phys.* **55**, 4789 (1971).

32. P. Saxe, D. J. Fox, H. F. Schaefer and N. C. Handy, *J. Chem. Phys.* **77**, 5584 (1982).

33. S. R. Langhoff and E. R. Davidson, *Int. J. Quantum Chem.* **8**, 61 (1974).

34. E. R. Davidson, in *The World of Quantum Chemistry*, edited by R. Daudel and B. Pullman (Reidel, Dorrecht), 1974, p. 17.

35. G. E. Scuseria, *Chem. Phys. Lett.* **176**, 27 (1991).

36. G. D. Purvis and R. J. Bartlett, *J. Chem. Phys.* **76**, 1910 (1982).

37. G. E. Scuseria, C. L. Janssen and H. F. Schaefer, *J. Chem. Phys.* **89**, 7382 (1988).

38. K. Raghavachari, G. W. Trucks, J. A. Pople and M. Head-Gordon, *Chem. Phys. Lett.* **157**, 479 (1989).

39. G. Herzberg, in *Molecular Spectra and Molecular Structure III Electronic Spectra and Electronic Structure of Polyatomic Molecules*, (Krieger), 1991, p. 629.

40. G. S. Hammond, *J. Am. Chem. Soc.* **77**, 334 (1955).

41. Y. Yamaguchi and H. F. Schaefer, *J. Chem. Phys.* **73**, 2310 (1980).

42. Y. Yamaguchi, M. J. Frish, J. F. Gaw, H. F. Schaefer and J. S. Binkley, *J. Chem. Phys.* **84**, 2262 (1986).

43. B. H. Besler, G. E. Scuseria, A. C. Scheiner and H. F. Schaefer, *J. Chem. Phys.* **89**, 360 (1988).

44. J. R. Thomas, B. J. DeLeeuw, G. Vacek and H. F. Schaefer, *J. Chem. Phys.* **98**, 1336 (1993).

45. J. R. Thomas, B. J. DeLeeuw, G. Vacek, T. D. Crawford, Y. Yamaguchi and H. F. Schaefer, *J. Chem. Phys.* **99**, 403 (1993).

46. R. M. Badger, *J. Chem. Phys.* **2**, 128 (1934); **3**, 710 (1935).

47. D. Demoulin, *Chem. Phys.* **11**, 329 (1975).

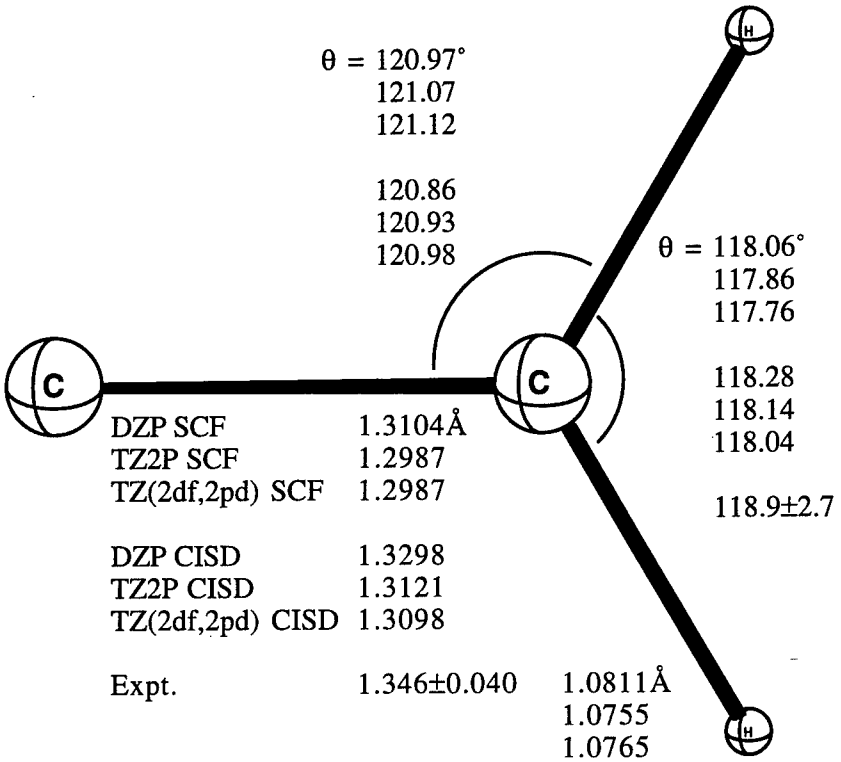

Figure 1: Predicted Structure of ã $^3B_2$ Vinylidene.

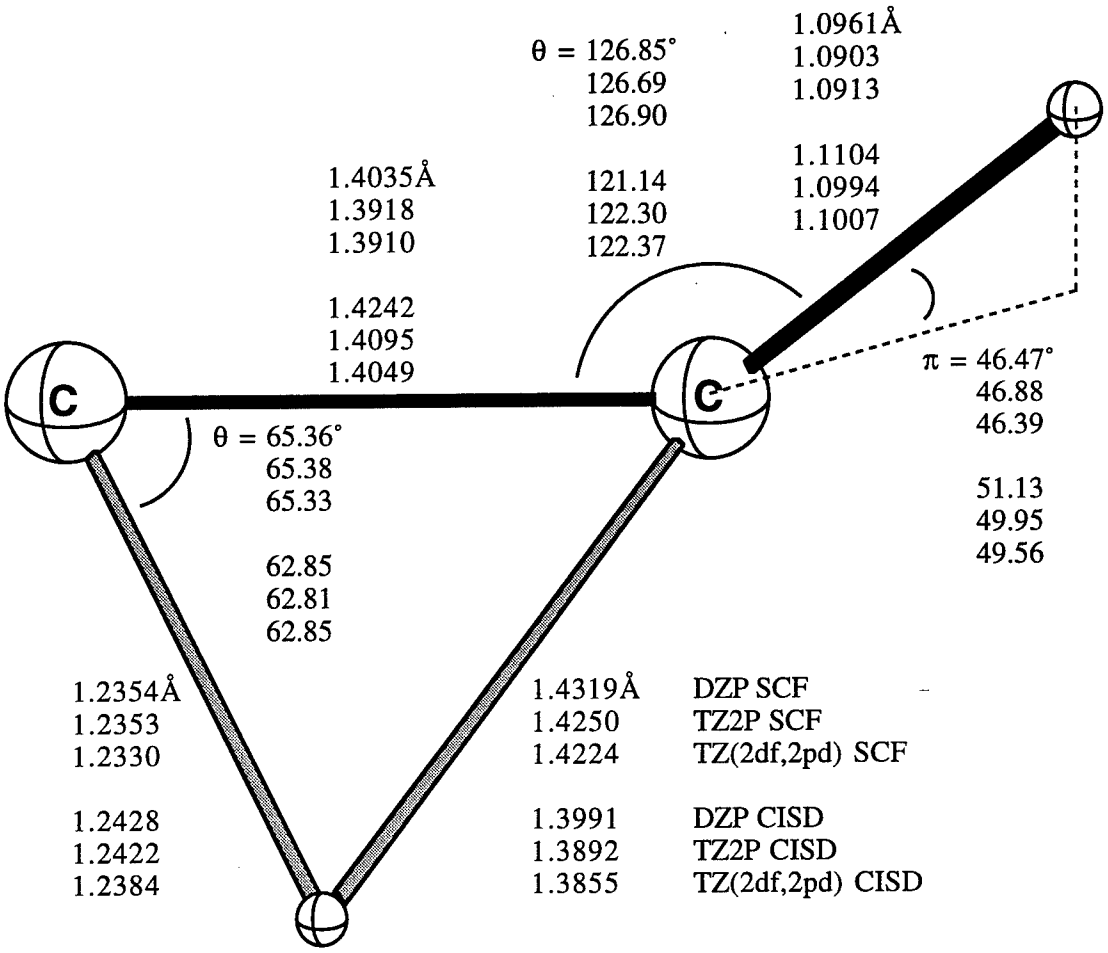

Figure 2: Predicted Structure of C_1-symmetry Transition State for the $^3B_2$ Vinylidene ↔ ^3B_u *trans*-bent Acetylene Isomerization Reaction.

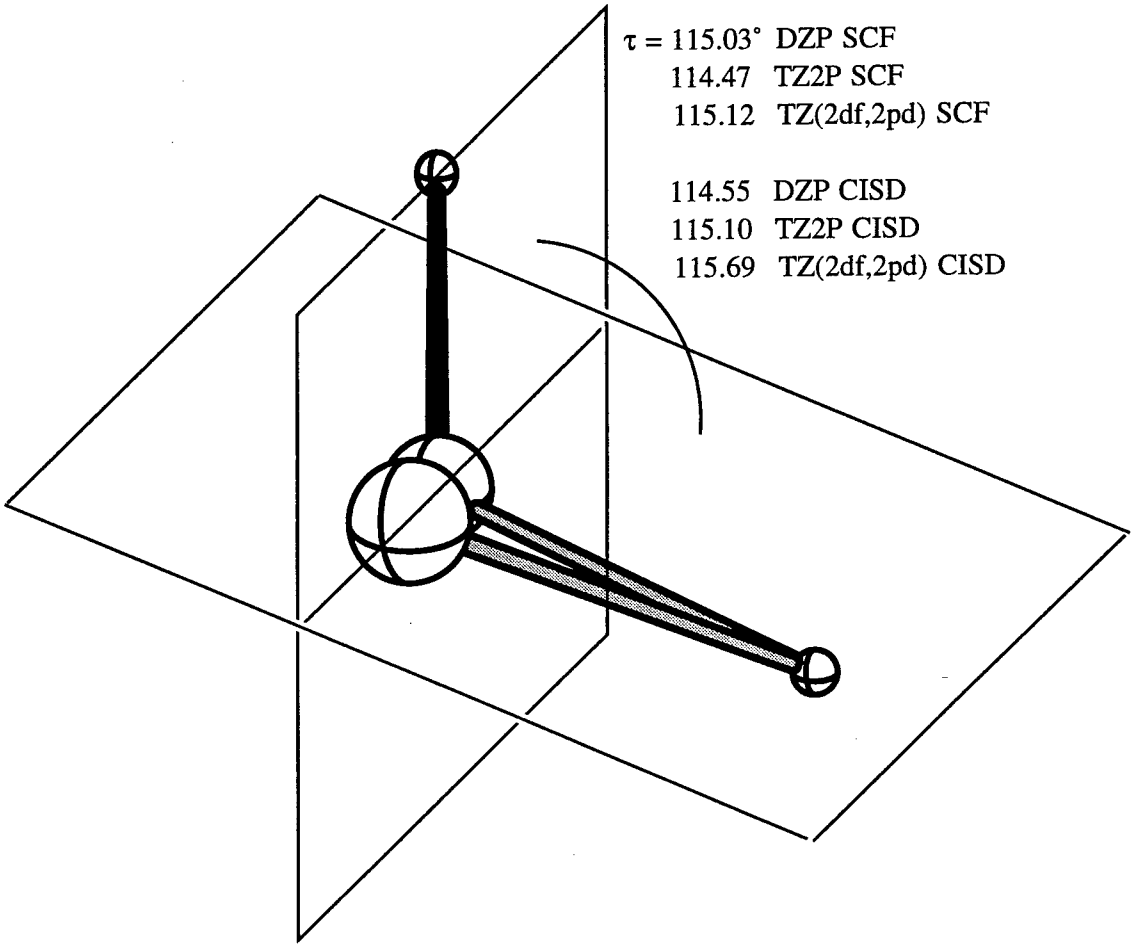

Figure 3: Predicted Torsional Angle of the C_1-symmetry Transition State for the $^3B_2$ Vinylidene $\leftrightarrow$ ^3B_u *trans*-bent Acetylene Isomerization Reaction.

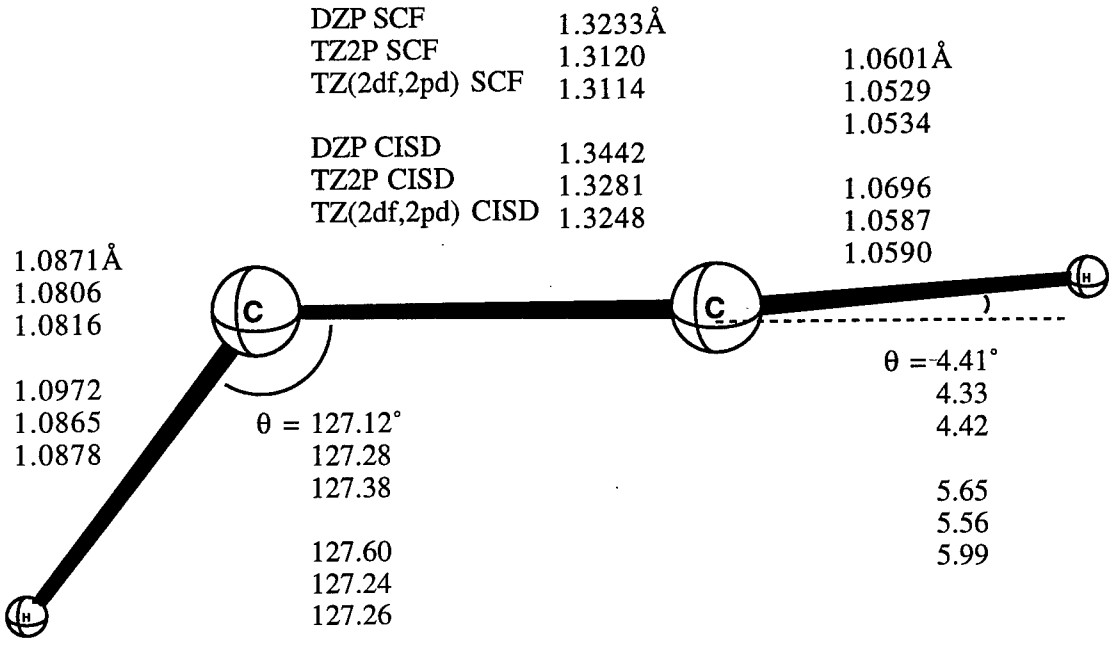

Figure 4: Predicted Structure of C_s-symmetry Transition State for the ^3B_u *trans*-bent ↔ $^3B_2$ *cis*-bent Acetylene Isomerization Reaction.

Table I. Theoretical predictions of the total energy (in hartrees), dipole moment (in debye), harmonic vibrational frequencies (in cm^{-1}), infrared (IR) intensities (in $km \cdot mol^{-1}$) and zero point vibrational energy (ZPVE) (in $kcal \cdot mol^{-1}$) for the $\tilde{a}\ ^3B_2$ state of vinylidene.

			Harmonic Vibrational Frequency/IR Intensities						
Level of Theory	Energy	μ	a_1	a_1	a_1	b_1	b_2	b_2	ZPVE
DZP SCF	-76.728 137	0.465	3274/6	1743/<1	1529/6	969/18	3368/9	1090/2	17.12
TZ2P SCF	-76.741 061	0.425	3255/6	1744/<1	1540/6	993/18	3338/6	1095/1	17.10
TZ(2df,2pd) SCF	-76.743 263	0.428	3240/6	1743/<1	1535/6	996/18	3323/7	1092/1	17.05
DZP CISD	-76.954 559	0.605	3173/5	1623/3	1454/3	790/9	3269/10	1033/3	16.21
TZ2P CISD	-76.989 205	0.556	3152/5	1625/3	1456/3	841/9	3237/4	1033/1	16.22
TZ(2df,2pd) CISD	-77.012 109	0.571	3143/4	1637/3	1451/4	853/8	3242/4	1027/<1	16.23
Expt.[a]			2930	1530	1375				

[a]Experimental fundamental frequencies are taken from reference 6. Reported experimental error bars are ± 10 cm^{-1}, ± 70 cm^{-1} and ± 10 cm^{-1}, respectively.

Table IIa. Theoretical predictions of the harmonic vibrational frequencies (in cm^{-1}) for $\tilde{a}\ ^3B_2$ state of d_1-vinylidene.

		Harmonic Vibrational Frequency					
Species	Level of Theory	CD s-stre	CC stre	CD_2 sciss.	CD as-stre	CD_2 rock	out of pl.
$D_2C=C$:	DZP SCF	2386	1699	1119	2509	858	772
	TZ2P SCF	2372	1699	1127	2485	863	792
	TZ(2df,2pd) SCF	2361	1698	1123	2474	860	794
	DZP CISD	2305	1588	1063	2435	813	630
	TZ2P CISD	2289	1590	1064	2410	814	671
	TZ(2df,2pd) CISD	2284	1604	1058	2423	806	680
	Expt.[a]	2160	1495	1010			

[a]Experimental *fundamental* frequencies are taken from reference 6. Reported experimental error bars are ± 10 cm^{-1}.

Table IIb. Theoretical predictions of the harmonic vibrational frequencies (in cm^{-1}) for ã $^3B_2$ state of d_2-vinylidene.

		Harmonic Vibrational Frequency					
		CH stre	CD stre	CC stre	CCH bend	CCD bend	out of pl.
H D C = C :	DZP SCF	3324	2444	1720	1388	917	876
	TZ2P SCF	3299	2425	1721	1397	922	898
	TZ(2df,2pd) SCF	3284	2414	1719	1392	919	901
	DZP CISD	3224	2366	1605	1319	869	714
	TZ2P CISD	3197	2346	1607	1320	869	761
	TZ(2df,2pd) CISD	3197	2349	1620	1313	863	771
	Expt.[a]	2960	2195	1510	1245	835	

[a]Experimental *fundamental* frequencies are taken from reference 6. Reported experimental error bars are ± 10 cm^{-1}.

Table III. Theoretical predictions of the total energy (in hartrees), dipole moment (in debye), harmonic vibrational frequencies (in cm^{-1}), and zero point vibrational energy (ZPVE) (in kcal/mole) for the C_1-symmetry transition state between $\tilde{a}\ ^3B_2$ vinylidene and $\tilde{b}\ ^3B_u$ acetylene.

			Harmonic Vibrational Frequency						
Level of Theory	Energy	μ	ω_1	ω_2	ω_3	ω_4	ω_5	ω_6	ZPVE
DZP SCF	-76.631 361	2.941	3149	2354	1463	1023	843	1777*i*	12.63
TZ2P SCF	-76.644 402	2.932	3120	2314	1448	1037	815	1729*i*	12.49
TZ(2df,2pd) SCF	-76.647 045	2.915	3106	2337	1457	1034	836	1731*i*	12.54
DZP CISD	-76.863 831	2.166	2997	2340	1343	948	775	1494*i*	12.01
TZ2P CISD	-76.897 256	2.271	2974	2259	1324	953	758	1504*i*	11.82
TZ(2df,2pd) CISD	-76.921 912	2.272	2970	2316	1355	955	777	1500*i*	11.97

Table IV. Theoretical predictions of the total energy (in hartrees), dipole moment (in debye), harmonic vibrational frequencies (in cm^{-1}), and zero point vibrational energy (ZPVE) (in kcal/mole) for the C_s-symmetry transition state between $\tilde{a}\ ^3B_2$ acetylene and $\tilde{b}\ ^3B_u$ acetylene.

			Harmonic Vibrational Frequency						
			ω_1	ω_2	ω_3	ω_4	ω_5	ω_6	
Level of Theory	Energy	μ	a'	a'	a'	a'	a'	a"	ZPVE
DZP SCF	-76.704 337	0.767	3610	3239	1724	1132	1144*i*	698	14.87
TZ2P SCF	-76.717 607	0.739	3601	3213	1716	1135	1155*i*	713	14.84
TZ(2df,2pd) SCF	-76.720 226	0.740	3597	3200	1721	1133	1147*i*	739	14.85
DZP CISD	-76.930 985	0.740	3497	3130	1616	1081	1022*i*	543	14.32
TZ2P CISD	-76.966 887	0.720	3486	3103	1609	1077	1026*i*	553	14.05
TZ(2df,2pd) CISD	-76.991 197	0.720	3504	3099	1633	1069	995*i*	627	14.20

Table V. The CISD+Q, CCSD, and CCSD(T) total energies[a] (in hartrees) for the $\tilde{a}\ ^3B_2$ state of vinylidene, the C_1-symmetry transition state for the $\tilde{a}\ ^3B_2$ vinylidene $\tilde{b}$ *trans*-bent ^3B_u acetylene isomerization reaction, and the C_s-symmetry transition state for the $\tilde{a}\ ^3B_2$ *cis*-bent acetylene $\tilde{b}\ ^3B_u$ *trans*-bent acetylene isomerization reaction.

Level of Theory	Minimum $\tilde{a}\ ^3B_2$ vinylidene	Transition State C_1-symmetry	Transition State C_s-symmetry
DZP CISD+Q	-76.976 856	-76.887 791	-76.953 322
TZ2P CISD+Q	-77.013 721	-76.923 670	-76.991 530
TZ(2df,2pd) CISD+Q	-77.038 453	-76.950 316	-77.017 634
DZP CCSD	-76.972 966	-76.885 855	-76.949 182
TZ2P CCSD	-77.009 366	-76.921 416	-76.986 781
TZ(2df,2pd) CCSD	-77.033 857	-76.948 062	-77.012 613
DZP CCSD(T)	-76.981 422	-76.896 612	-76.958 916
TZ2P CCSD(T)	-77.020 858	-76.935 364	-76.999 235
TZ(2df,2pd) CCSD(T)	-77.046 808	-76.963 704	-77.026 330

[a]CISD+Q, CCSD and CCSD(T) energies were evaluated at the CISD optimized geometries for the same basis set.

Table VI. Relative Energies[a] (in kcal/mole) for the triplet acetylene/vinylidene potential energy hypersurface.

Level of Theory	ã $^3B_2$ Acet[b]	C_s-symm trns st	$\tilde{b}$ ^3B_u Acet[b]	C_1-symm trns st	ã $^3B_2$ Vinylidene
DZP SCF	0.00	17.31 (15.81)	7.48 (7.62)	63.10 (59.36)	2.37 (3.12)
TZ2P SCF	0.00	17.16 (15.68)	7.31 (7.46)	63.09 (59.26)	2.44 (3.22)
TZ(2df,2pd) SCF	0.00	17.02 (15.57)	7.39 (7.53)	62.94 (59.18)	2.56 (3.31)
DZP CISD	0.00	16.24 (15.05)	8.20 (8.49)	58.38 (54.88)	1.45 (2.15)
TZ2P CISD	0.00	15.53 (14.15)	7.86 (8.18)	59.22 (55.61)	1.53 (2.32)
TZ(2df,2pd) CISD[c]	0.00	15.25 (13.96)	8.17 (8.41)	74.20 (70.68)	2.13 (2.87)
DZP CISD+Q	0.00	15.73 (14.54)	8.07 (8.36)	56.85 (53.35)	0.96 (1.66)
TZ2P CISD+Q	0.00	15.04 (13.66)	7.84 (8.16)	57.62 (54.01)	1.11 (1.90)
TZ(2df,2pd) CISD+Q[c]	0.00	14.81 (13.52)	8.23 (8.47)	57.06 (53.54)	1.75 (2.49)
DZP CCSD	0.00	15.54 (14.35)	7.98 (8.27)	55.28 (51.78)	0.61 (1.31)
TZ2P CCSD	0.00	14.90 (13.52)	7.75 (8.07)	55.91 (52.30)	0.72 (1.51)
TZ(2df,2pd) CCSD[c]	0.00	14.68 (13.39)	8.14 (8.38)	55.18 (51.66)	1.35 (2.09)
DZP CCSD(T)	0.00	15.00 (13.81)	7.68 (7.97)	54.10 (50.60)	0.88 (1.58)
TZ2P CCSD(T)	0.00	14.48 (13.10)	7.59 (7.91)	54.56 (50.95)	0.91 (1.70)
TZ(2df,2pd) CCSD(T)[c]	0.00	14.33 (13.04)	8.03 (8.27)	53.62 (50.10)	1.48 (2.22)

[a]Numbers in parentheses include zero point vibrational energy (ZPVE) corrections. CISD+Q, CCSD and CCSD(T) energies were determined at the CISD optimized geometries and corrected using CISD ZPVE corrections with the same basis set.

[b]Energies for $\tilde{a}\ ^3B_2$ and $\tilde{b}\ ^3B_u$ acetylene were taken from reference 20.

[c]The ZPVE correction for $\tilde{a}\ ^3B_2$ and $\tilde{b}\ ^3B_u$ acetylene was obtained in this work for the TZ(2df,2pd) basis set (see Appendix A).

Table VII. Theoretical predictions for the $\tilde{X}\ ^1A_1$- $\tilde{a}\ ^3B_2$ vinylidene energy separation (in kcal/mole)[a,b].

Level of Theory	$T_e(\tilde{X}\ ^1A_1$- $\tilde{a}\ ^3B_2)$	$T_0(\tilde{X}\ ^1A_1$- $\tilde{a}\ ^3B_2)$
DZP SCF	31.37	32.31
TZ2P SCF	32.79	33.76
TZ(2df,2pd) SCF	32.89	33.86
DZP CISD	40.70	41.56
TZ2P CISD	42.36	43.30
TZ(2df,2pd) CISD	43.75	44.73
DZP CISD+Q	41.45	42.31
TZ2P CISD+Q	43.53	44.47
TZ(2df,2pd) CISD+Q	45.16	46.14
DZP CCSD	41.21	42.06
TZ2P CCSD	43.18	44.12
TZ(2df,2pd) CCSD	44.76	45.74
DZP CCSD(T)	41.76	42.61
TZ2P CCSD(T)	43.93	44.87
TZ(2df,2pd) CCSD(T)	45.58	46.56
Expt.[b]	46.8 ± 0.5	47.60 ± 0.14

[a]CISD+Q, CCSD and CCSD(T) energies were determined at the CISD optimized geometries, and the CISD ZPVE corrections with the same basis set were used. Where possible, energies for $\tilde{X}\ ^1A_1$ vinylidene were taken from reference 7. The rest were obtained in this work (see Appendix A).

[b]The experimentally measured values are taken from reference 6.

Chapter III

The $\tilde{X}$ AlOH - $\tilde{X}$ HAlO Isomerization Potential Energy Hypersurface[1]

[1] G. Vacek, B. J. DeLeeuw and H. F. Schaefer *J. Chem. Phys.* **98**, 8704 (1993).

Ab initio molecular electronic structure theory has been used to study the AlOH–HAlO unimolecular isomerization reaction on the singlet ground state potential energy surface. Electron correlation effects were included via configuration interaction and coupled-cluster methods. Basis sets as complete as triple zeta plus two sets of polarization functions and a set of higher angular momentum functions [TZ(2df,2pd)] were employed. The *classical* barrier for hydrogen migration from $\tilde{X}$ HAlO to $\tilde{X}$ AlOH is predicted to be 38.4 kcal mol^{-1} using the TZ(2df,2pd) basis set with the coupled-cluster method including all single and double excitations with the effect of connected triple excitations included perturbatively [CCSD(T)]. After correction for zero-point vibrational energies (ZPVEs), an activation energy of 36.6 kcal mol^{-1} is obtained. The ΔE for isomerization is -42.2 (-40.5 with ZPVE correction) kcal mol^{-1} at the same level of theory. The dipole moments of HAlO and AlOH in their equilibrium geometries are 4.525 and 1.040 debye, respectively, at the same level of theory. A comparison is also made between a theoretically predicted harmonic vibrational frequency and a recently determined experimental fundamental frequency for $\tilde{X}$ AlOH.

Introduction

Metal hydroxides are often the result of metal atom insertion or elimination reactions with water in environments undergoing metal ablation, sputtering or combustion. The simplest of these, metal monohydroxides, form a class of molecules upon which to test elementary concepts of chemical bonding. Nonlinearity of metal hydroxides is thought to indicate the extent to which the metal-hydroxide bond is covalent rather than ionic. Covalent bonding tends to favor bent structures (e.g. H_2O, BOH[1]), while ionic bonding favors linear structures (e.g. CaOH,[2] SrOH,[3] BaOH[4]). MgOH,[5] which is quasilinear, may be considered to have an ionic bond with covalent features. Evidence suggests that the linearity, nonlinearity, or quasilinearity of a molecule may be qualitatively predicted from simple electronegativity arguments. Atoms such as B and Cu with electronegativities near that of hydrogen (2.2) form bent monohydroxides.[1,6] Atoms with electronegativities near

or below 1, like most alkali metals[7,8] and alkaline earths,[2-4] turn out to be linear. Mg has an electronegativity between these two extremes (1.31), and MgOH turns out to be quasilinear.[5] Al has an electronegativity of 1.61, so AlOH might also expected to be quasilinear.

Recently, the first observation of an electronic spectrum for $\tilde{X}$ AlOH has been reported by Pilgrim, Robbins and Duncan.[9] The presumed structure and bonding of the system was also discussed. Since they produced the subject of their research through aluminum insertion into water, it was initially unclear whether their spectrum should be assigned to the AlOH or HAlO isomer. Previous theoretical studies,[10,11] mass-spectrometric analyses,[12] and infrared[13] (IR) and optical[14] assignments did not provide sufficient information about the relative stabilities and the vibrational frequencies of these two species for them to make a satisfactory assignment. Here we present results of our inquiry into the isomerization reaction from $\tilde{X}$ AlOH to $\tilde{X}$ HAlO and the associated potential energy surface (PES). Some of the data reported herein was crucial to Pilgrim *et al.*'s[9] assignments. We are confident that it will be helpful to future experimental studies of these two interesting isomers.

Theoretical Methods

Three different basis sets were used in this research. The double zeta plus polarization basis (DZP) is a standard Huzinaga-Dunning-Hay[15,16] double-ζ set of contracted Gaussian functions augmented by a set of six Cartesian d-like polarization functions on oxygen [α_d(O) = 0.85] and aluminum [α_d(Al) = 0.40] and a set of p-type polarization functions on hydrogen [α_p(H) = 0.75]. The contraction scheme for the DZP basis is thus:

Al(11s7p1d/6s4p1d); O(9s5p1d/4s2p1d); H (4s1p/2s1p).

The triple zeta plus double polarization basis (TZ2P) is triple-ζ in the valence region and adds two sets of polarization functions per atom [α_d(Al) = 0.8, 0.2; α_d(O) = 1.7, 0.425;

α_p(H) = 1.5, 0.375]. For hydrogen and oxygen, standard Huzinaga-Dunning[15,17] sets of contracted Gaussian functions were used. For aluminum, McLean and Chandler's[18] contraction of Huzinaga's 12s9p primitive Gaussian set was used. The contraction scheme for the TZ2P basis is as follows:

Al (12s9p2d/6s5p2d); O (10s6p2d/5s3p2d); H (5s2p/3s2p).

The TZ(2df,2pd) basis was formed by adding a set of higher angular momentum polarization functions [α_f(Al) = 0.25; α_f(O) = 1.4; and α_d(H) = 1.0] to the TZ2P basis.

The restricted Hartree-Fock self-consistent field (SCF) method was initially employed in this study. The effects of electron correlation were taken into account using the method of configuration interaction including all single and double excitations from an SCF reference wavefunction (CISD), the coupled-cluster method including all single and double excitations (CCSD), and the CCSD method with the effect of connected triple excitations included perturbatively [CCSD(T)]. The two lowest (aluminum and oxygen 1s-like) SCF molecular orbitals were constrained to be doubly-occupied and the corresponding two highest virtual orbitals were deleted from the correlation procedure. With the TZ(2df,2pd) basis, this resulted in a total of 72,311 configurations in C_{2v} symmetry and 138,919 configurations in C_s symmetry.

The structures of ground state AlOH, HAlO, and the transition state connecting them via hydrogen migration were fully optimized using closed-shell analytic gradient techniques at the SCF,[19-21] CISD,[22-24] CCSD,[25] and CCSD(T)[26] levels of theory. Harmonic vibrational frequencies were obtained using analytic SCF second-derivative techniques[27-29] and central finite differences of analytic CISD, CCSD, and CCSD(T) gradients.

Relative energies designated CISD+Q were obtained for the various isomers studied here by adding the Davidson correction[30,31] for unlinked quadruple excitations to the CISD energy.

Discussion

Geometry

Walsh's rules[32] predict that both AlOH and HAlO should have linear ground state structures, just like the isovalent molecules HCN and HNC. Furthermore, it can be expected from the same rules that the lowest excited states of AlOH and HAlO should be bent and have similar bond angles. However, even in the simple case of the excited states of HCN and HNC, it has been shown[33] that Walsh concepts are not well followed.

As shown in Figure 1, the use of a DZP quality basis set leads to the prediction of a linear $\tilde{X}$ AlOH structure with all theoretical methods employed here. Previous theoretical results[10,11] also predicted AlOH to be linear using basis sets similar in extent to our DZP basis. However, with the more complete TZ2P basis set, we predict a geometry that is quite bent (~151°). This *qualitative* difference between the DZP and TZ2P equilibrium $\tilde{X}$ AlOH geometries implies that the use of still larger basis sets is desirable. It is not uncommon for a basis set with extensive character in the *spd* space but no higher angular momentum functions to prefer, somewhat erroneously, a bent geometry over a linear one.[34,35] In such cases, further study with basis sets which do incorporate *f*-type functions will usually lead to an accurate prediction of both geometry and harmonic vibrational frequencies.[36,37]

Thus, our best prediction of the equilibrium geometry of AlOH is at the TZ(2df,2pd) CCSD(T) level of theory, where the bond angle is predicted to be 162.6°. At this level of theory, we see essentially a hydroxide group with a tight single bond (r_e(OH) = 0.951 Å). The experimentally estimated value of $r_e(OH^-)$ lies within 0.001 Å[38] of the r_e(OH) value, 0.970 Å.[39] This "hydroxide group" is ionically bonded to the partially positive Al atom (r_e(AlO) = 1.682 Å). Plots of the 9a' molecular orbital (MO) show that it is essentially a lone pair of electrons in an Al 3*s* orbital slightly polarized along the molecular axis by the Al $3p_z$ orbital to produce a weak sigma type interaction between this "lone pair" and the hydroxide group.

It is important to note that despite the bent equilibrium geometry of AlOH, it can at best be referred to as quasilinear. For many of the levels of theory utilized in this paper, barriers to linearity were calculated. In all cases, the predicted barrier to linearity was less than 1 kcal mol^{-1}. Thus the ZPVE is greater than the linearity barrier. In many experimental set-ups, the "averaged" linear geometry would be observed. The predicted bond angle is significantly larger than that predicted for $\tilde{X}$ BOH (θ_e = 125°),[1] which has a truly bent structure. This structural difference between AlOH and BOH is in agreement with the qualitative predictions based upon electronegativities mentioned in the introduction.

The structure of $\tilde{X}$ HAlO, depicted in Figure 2, was predicted to be linear at all levels of theory, in accordance with Walsh's rules.[32] The best results, at the TZ(2df,2pd) CCSD(T) level of theory, show r_e(AlH) = 1.562 Å and r_e(AlO) = 1.608 Å. The AlH bond distance is somewhat short compared to the 1.6478 Å bond length of diatomic AlH.[39] Presumably, this is due to the greater *s* character within the AlH bond of HAlO as compared to that of the diatomic. According to Huber and Herzberg,[39] the bond length of the AlO diatomic molecule (with a bond order of 2.5) is 1.6179 Å.

Figure 3 shows the transition state for the hydrogen migration from AlOH to HAlO. The hydrogen is closer to Al than O, which agrees nicely with Hammond's Postulate for endothermic reactions,[40] since HAlO is much higher in energy than AlOH. The best description of the transition state structure should again be the TZ(2df,2pd) CCSD(T) results.

Harmonic Vibrational Frequencies

Typically, the harmonic vibrational frequencies of a molecule are only predicted accurately at levels of theory where the predicted geometry is qualitatively correct. We suspect that only the frequencies predicted with the TZ(2df,2pd) basis set and reasonable

levels of electron correlation will thus be accurate to an acceptable degree. Specifically, we expect the TZ(2df,2pd) CCSD(T) level of theory to give excellent results.[37]

At the TZ(2df,2pd) CCSD(T) level of theory, our predictions of the harmonic vibrational frequencies of AlOH, found in Table I, are 4017, 845 and 155 cm^{-1} for the OH stretching, AlO stretching, and the bending frequencies. The only experimentally assigned fundamental vibrational frequency in the gas phase is that of Pilgrim.[9] A $\Delta G_{1/2}$ value of 895 cm^{-1} was tentatively assigned to the AlO stretching mode. This is higher than our prediction, but the agreement is still acceptable. It is also conceivable that Pilgrim observed a combination band of the AlO stretch and the AlOH bend. The sum of our harmonic vibrational predictions is 1000 cm^{-1}, nicely above Pilgrim's 895 cm^{-1} fundamental. Our predictions for the two harmonic stretching vibrational frequencies are also in satisfactory agreement with the fundamental stretching frequencies of Hauge *et al.*[13] (ν_1 = 3790, ν_2 = 810 cm^{-1}), which were measured in a noble gas matrix. The disagreement between these two experimental ν_2 assignments is somewhat surprising.

For the HAlO conformer, Table II, the TZ(2df,2pd) CCSD(T) harmonic vibrational frequencies are predicted to be 2002, 1056 and 400 cm^{-1} for the AlH stretching mode, the AlO stretching mode and the bending mode, respectively. These predicted values do not match well with Pilgrim's[9] results, thus supporting his assignment to AlOH rather than HAlO.

There are no experimental vibrational frequency assignments for HAlO. Huber and Herzberg[39] list experimental harmonic vibrational frequency assignments for the diatomic molecules AlH and AlO as 1683 and 979 cm^{-1}, respectively. The HAlO molecule has an AlO stretch harmonic vibrational frequency that looks just slightly perturbed from that of diatomic AlO.

Harmonic vibrational frequencies for the isotopically-substituted ground states are presented in Tables III and IV. Comparison between predicted harmonic and experimentally assigned fundamentals are favorable for AlOD. The only isotopic shift for

AlOD that is determinable from experimental results is $\Delta\nu_2$ = 15.1 cm^{-1} by Hauge.[13] The predicted isotopic shift agrees well at all levels of theory, e.g. 18 cm^{-1} for TZ(2df,2pd) CCSD(T). Hauge[13] also reports that ν_2(Al^{18}O) = 785.2 cm^{-1}, shifted 25.1 cm^{-1}. Our theoretical predictions, not tabulated here, agree well with this experimental assignment. For TZ(2df,2pd) CCSD(T) we predict ω_e(Al^{18}O) = 817 cm^{-1}, a shift of 28 cm^{-1}. There are no experimental isotopic vibrational assignments for DAlO, but we are confident that our predictions are good.

Table V shows the harmonic vibrational frequencies of the transition state for hydrogen migration. At the TZ(2df,2pd) CCSD(T) level of theory, the real vibrational modes have the magnitudes 1755 cm^{-1} and 909 cm^{-1}, while the imaginary mode has a magnitude of 945*i* cm^{-1}.

Energetics

Relative energies of $\tilde{X}$ AlOH, $\tilde{X}$ HAlO, and the transition state are given in Table VI. At the highest level of theory used here [TZ(2df,2pd) CCSD(T)], AlOH is more stable than HAlO by 42.2 kcal mol^{-1}. At the same level of theory the classical barrier to hydrogen migration from $\tilde{X}$ AlOH to $\tilde{X}$ HAlO is found to be 80.5 kcal mol^{-1}, while zero-point vibrational energy (ZPVE) corrections give an activation energy of 77.2 kcal mol^{-1}. Thus, AlOH is extremely stable with respect to isomerization once produced. Although the HAlO to AlOH isomerization reaction is strongly exothermic with ΔE = -42.2 (-40.5 with ZPVE) kcal mol^{-1}, the barrier height for $\tilde{X}$ HAlO to $\tilde{X}$ AlOH isomerization is 38.4 (36.6 with ZPVE) kcal mol^{-1}. If it were generated, HAlO should be observable because of its kinetic stability with respect to isomerization.

Interestingly, the PES in the related case of $\tilde{X}$ HBO $\leftrightarrow$ $\tilde{X}$ BOH[1,11] isomerization is almost the exact opposite of that predicted here for HAlO and AlOH. That is, the trivalent HBO isomer is ~40 kcal mol^{-1} more stable than the monovalent BOH isomer, and the transition state connecting them is ~50 kcal mol^{-1} above BOH.[1] In many ways, first-row

elements such as boron are oddities and stand apart from the heavier elements in their respective groups. When moving down the periodic table within Group 13 (B, Al, Ga, In, Tl), the monovalent state becomes progressively more stable.[41] One explanation for this trend and the predicted monovalent AlOH ground state is the inert *s*-pair effect. Kutzelnigg[42] has noted that the 2*s* and 2*p* orbitals of first-row elements are uniquely well suited for hybridization because they have similar spatial extent. First-row elements have only *s*-type core electrons. As a result, their valence *p* orbitals are relatively compact. Elements in higher rows have cores that contain both *s*- and *p*-type electrons; their valence *p* orbitals are substantially more diffuse than their valence *s* orbitals, and hybridization is much less efficient.

Recall that the chemistry of lower Group 14 elements (Si, Ge, etc.) is often radically different from that of carbon; this has been explained in terms of increasing stability of the divalent state while moving downward within the group. The divalent state stabilization energy (DSSE), defined to be the difference between the first and second bond dissociation energies, is a convenient way to express this trend. For example, DSSE(CH_2) = -5.6 kcal mol^{-1}, while DSSE(SiH_2) = +19.3 kcal mol^{-1} and DSSE(GeH_2) = +25.8 kcal mol^{-1}. The usefulness of DSSEs with respect to Group 14 chemistry has been discussed elsewhere by Grev.[43] Using G2 theory thermochemical data,[44] the equivalent "monovalent state stabilization energy" may be determined for both BH (-28.8 kcal mol^{-1}) and AlH (+39.6 kcal mol^{-1}). Although this treatment of the thermochemistry is hardly complete, it does provide a strong indication that the monovalent structure (MOH) should be much more favorable relative to the trivalent structure (OMH) in the case of Al as opposed to B.

Conclusion

The singlet ground state PES for the AlOH-HAlO isomerization reaction has been studied with ab initio molecular electronic structure theory. AlOH was found to be

quasilinear with an equilibrium bond angle of 162.6° contrary to Walsh's rules. Predictions herein for AlOH compare favorably with recently determined experimental results. Agreement is sufficient to confirm the experimental assignments. HAlO was linear at all levels of theory in agreement with Walsh.

At the [TZ(2df,2pd)] CCSD(T) level of theory, the classical barrier for $\tilde{X}$ HAlO to $\tilde{X}$ AlOH rearrangement is predicted to be 38.4 kcal mol^{-1}, while it is 36.6 kcal mol^{-1} with ZPVE corrections. The ΔE for this isomerization reaction is -42.2 (-40.5 with ZPVE) kcal mol^{-1} at that level of theory. The AlOH conformation lies lowest on the AlOH-HAlO PES, in stark contrast with the HBO global minimum on the BOH-HBO PES. This apparent lack of periodicity within Group 13 can be explained in terms of the increasing stability of the monovalent state for lower elements in that group.

Acknowledgment

This research was supported by the Air Force Office of Scientific Research, Grant No. AFOSR-88-0167. This material is based upon work supported under NSF and DOD Graduate Fellowships. The authors would like to thank Roger Grev for helpful discussions and Jeff Pilgrim, Dave Robbins and Professor Michael Duncan for providing their experimental results prior to publication. GV and BJD would also like to point out that they are hoping for yet another volleyball rematch with Duncan's Lazer Jox.

References

1. T. S. Zyubina, O. P. Charkin and L. V. Gurvich, *Zh. Strukt. Khim.* **20** (1979) 3.

2. R. C. Hilborn, Z. Qingshi and D. O. Harris, *J. Mol. Spectrosc.* **97** (1983) 73.

3. J. Nakagawa, R. F. Wormsbecher and D. O. Harris, *J. Mol. Spectrosc.* **97** (1983) 37.

4. S. Kinsey-Nielsen, C. R. Brazier and P. F. Bernath, *J. Chem. Phys.* **84** (1986) 698.

5. W. L. Barclay Jr., M. A. Anderson and L. M. Ziurys, *Chem. Phys. Lett.* **196** (1992) 225.

6. M. Trkula and D. O. Harris, *J. Chem. Phys.* **79** (1983) 1138.

7. D. R. Lide and R. L. Kuczkowski, *J. Chem. Phys.* **46** (1967) 4768.

8. C. Matsumura and D. R. Lide, *J. Chem. Phys.* **50** (1969) 71.

9. J. S. Pilgrim, D. L. Robbins and M. A. Duncan, *Chem. Phys. Lett.* **202** (1993) 203.

10. T. S. Zyubina, O. P. Charkin and L. V. Gurvich, *Zh. Strukt. Khim.* **20** (1979) 12.

11. T. S. Zyubina, A. S. Zyubina, A. A. Gorbik and O. P. Charkin, *Zh. Neorg. Khim.* **30** (1985) 2739.

12. M. I. Milushin, A. M. Emel'yanov and L. N. Gorokhov, *Teplofiz. Vys. Temp.* **20** (1979) 3.

13. R. H. Hauge, J. W. Kauffman and J. L. Margrave, *J. Am. Chem. Soc.* **102** (1980) 6005.

14. M. A. Douglas, R. H. Hauge and J. L. Margrave, *ACS Symp. Ser.* **179** (1982) 347.

15. S. Huzinaga, *J. Chem. Phys.* **42** (1965) 1293.

16. T. H. Dunning, *J. Chem. Phys.* **53** (1970) 2823.

17. T. H. Dunning, *J. Chem. Phys.* **55** (1971) 716.

18. A. D. McLean and G. S. Chandler, *J. Chem. Phys.* **72** (1980) 5639.

19. P. Pulay, in *Modern Theoretical Chemistry,* Vol. 4, edited by H. F. Schaefer (Plenum, New York), 1977, p. 153.

20. M. Dupuis and H. F. King, *J. Chem. Phys.* **68** (1978) 3998.

21. J. D. Goddard, N. C. Handy and H. F. Schaefer, *J. Chem. Phys.* **71** (1979) 1525.

22. B. R. Brooks, W. D. Laidig, P. Saxe, J. D. Goddard, Y. Yamaguchi and H. F. Schaefer, *J. Chem. Phys.* **72** (1980) 4652.

23. Y. Osamura, Y. Yamaguchi and H. F. Schaefer, *J. Chem. Phys.* **77** (1982) 383.

24. J. E. Rice, R. D. Amos, N. C. Handy, T. J. Lee and H. F. Schaefer, *J. Chem. Phys.* **85** (1986) 963.

25. A. C. Scheiner, G. E. Scuseria, J. E. Rice, T. J. Lee and H. F. Schaefer, *J. Chem. Phys.* **87** (1987) 5361.

26. G. E. Scuseria, *J. Chem. Phys.* **94** (1991) 442.

27. J. A. Pople, R. Krishnan, H. B. Schlegel and J. S. Binkley, *Int. J. Quantum. Chem.* **S13** (1975) 225.

28. P. Saxe, Y. Yamaguchi and H. F. Schaefer, *J. Chem. Phys.* **77** (1982) 5647.

29. Y. Osamura, Y. Yamaguchi, P. Saxe, D. J. Fox, M. A. Vincent and H. F. Schaefer, *J. Mol. Struct.* **103** (1983) 183.

30. S. R. Langhoff and E. R. Davidson, *Int. J. Quantum. Chem.* **8** (1974) 61.

31. E. R. Davidson, in *The World of Quantum Chemistry*, edited by R. Daudel and B. Pullman, (Reidel, Dordrecht), 1974, p. 17.

32. A. D. Walsh, *J. Chem. Soc.* (1953) 2288.

33. G. M. Schwenzer, H. F. Schaefer and C. F. Bender, *J. Chem. Phys.* **63** (1975) 569.

34. E. D. Simandiras, J. E. Rice, T. J. Lee, R. D. Amos and N. C. Handy, *J. Chem. Phys.* **88** (1988) 3187.

35. E. D. Simandiras, N. C. Handy and R. D. Amos, *J. Phys. Chem.* **92** (1988) 92.

36. J. R. Thomas, B. J. DeLeeuw, G. Vacek and H. F. Schaefer, *J. Chem. Phys.* **98** (1993) 1336.

37. J. R. Thomas, B. J. DeLeeuw, G. Vacek, T. D. Crawford, Y. Yamaguchi and H. F. Schaefer, *J. Chem. Phys.* **99** (1993) 403.

38. R. J. Celotta, R. A. Bennett and J. L. Hall, *J. Chem. Phys.* **60** (1974) 1740. H. Hotop, T. A. Patterson, and W. C. Lineberger, *J. Chem. Phys.* **60** (1974) 1806.

39. K. P. Huber and G. Herzberg, in *Constants of Diatomic Molecules*, Vol. 4 (Van Nostrand Reinhold), 1979, p. 24, 28, 508.

40. G. S. Hammond, *J. Am. Chem. Soc.* **77** (1955) 334.

41. F. A. Cotton and G. Wilkinson, in *Advanced Inorganic Chemistry*, Ed. 5 (Wiley), 1988, p. 208.

42. W. Kutzelnigg, *Angew. Chem., Int. Ed. Engl.* **23** (1984) 272.

43. R. S. Grev, *Adv. in Organometallic Chem.* **33** (1991) 125.

44. L. A. Curtiss, K. Raghavachari, G. W. Trucks and J. A. Pople, *J. Chem. Phys.* **94** (1991) 7221.

180.00°
150.36°
163.59°

180.00°
154.77°
168.70°

180.00°
151.50°
163.43°

180.00°
151.02°
162.59°

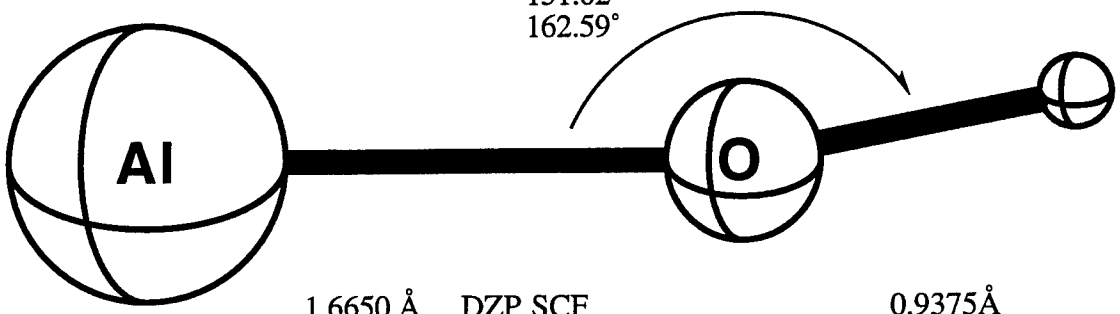

1.6650 Å	DZP SCF	0.9375Å
1.6734 Å	TZ2P SCF	0.9326Å
1.6634 Å	TZ(2df,2pd) SCF	0.9318Å
1.6763 Å	DZP CISD	0.9505Å
1.6830 Å	TZ2P CISD	0.9421Å
1.6702 Å	TZ(2df,2pd) CISD	0.9420Å
1.6813 Å	DZP CCSD	0.9555Å
1.6915 Å	TZ2P CCSD	0.9477Å
1.6782 Å	TZ(2df,2pd) CCSD	0.9478Å
1.6828 Å	DZP CCSD(T)	0.9568Å
1.6956 Å	TZ2P CCSD(T)	0.9506Å
1.6824 Å	TZ(2df,2pd) CCSD(T)	0.9508Å

Figure 1. Predicted equilibrium geometry for $\tilde{X}$ AlOH.

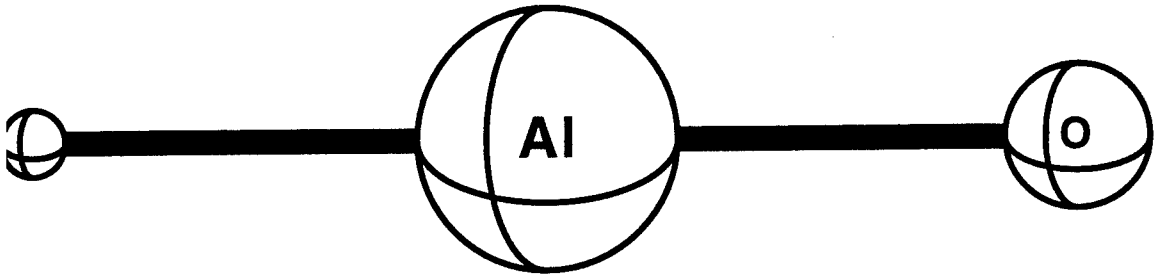

1.5480 Å	DZP SCF	1.5652 Å
1.5533 Å	TZ2P SCF	1.5658 Å
1.5542 Å	TZ(2df,2pd) SCF	1.5652 Å
1.5448 Å	DZP CISD	1.5891 Å
1.5526 Å	TZ2P CISD	1.5890 Å
1.5504 Å	TZ(2df,2pd) CISD	1.5849 Å
1.5500 Å	DZP CCSD	1.5996 Å
1.5606 Å	TZ2P CCSD	1.6006 Å
1.5584 Å	TZ(2df,2pd) CCSD	1.5963 Å
1.5535 Å	DZP CCSD(T)	1.6101 Å
1.5647 Å	TZ2P CCSD(T)	1.6126 Å
1.5623 Å	TZ(2df,2pd) CCSD(T)	1.6083 Å

Figure 2. Predicted equilibrium geometry for $\tilde{X}$ HAlO.

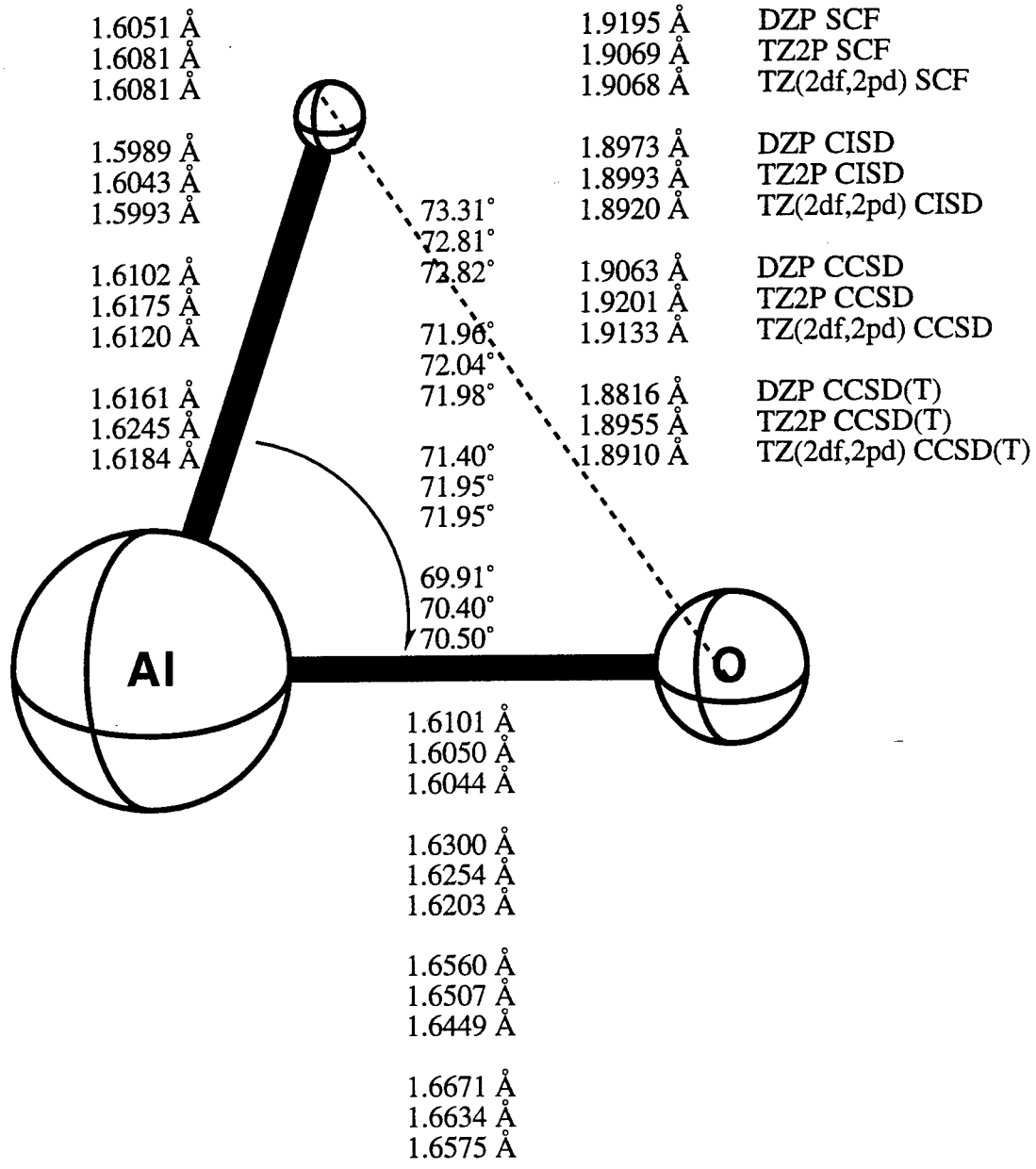

Figure 3. Predicted structure for C_s-symmetry transition state for the $\tilde{X}$ AlOH ↔ $\tilde{X}$ HAlO isomerization reaction.

Table I. Theoretical predictions of the total energy (in hartrees), dipole moment (in debye), harmonic vibrational frequencies (in cm^{-1}), infrared (IR) intensities (in $km \cdot mol^{-1}$) and zero-point vibrational energy (ZPVE) (in $kcal \cdot mol^{-1}$) for $\tilde{X}$ AlOH.

			Vibrational Frequencies /IR Intensities			
Level of Theory	Energy	μ	$\omega_1(a_1/a')^a$	$\omega_2(a_1/a')^a$	$\omega_3(e_1/a')^a$	ZPVE
DZP SCF	-317.417 730	1.355	4331/172	897/176	150/467	7.903
TZ2P SCF	-317.444 597	1.324	4298/123	871/153	257/177	7.757
TZ(2df,2pd) SCF	-317.447 545	1.318	4313/139	884/167	155/193	7.651
DZP CISD[b]	-317.745 905	1.134	4160/121	882/155	134/461	7.591
TZ2P CISD[b]	-317.819 728	1.127	4143/97	850/145	197/175	7.419
TZ(2df,2pd) CISD[b]	-317.848 834	1.097	4157/107	868/156	120/190	7.355
DZP CCSD	-317.773 831	1.027	4082/108	873/146	102/452	7.375
TZ2P CCSD	-317.853 004	1.098	4051/84	835/133	222/168	7.302
TZ(2df,2pd) CCSD	-317.884 083	1.045	4065/93	854/144	152/182	7.249
DZP CCSD(T)	-317.779 967	1.040	4057/100	869/137	79/446	7.267
TZ2P CCSD(T)	-317.864 170	1.099	4006/77	826/124	220/165	7.222
TZ(2df,2pd) CCSD(T)	-317.896 875	1.040	4017/85	845/135	155/179	7.173
Expt.[1]				$\nu_2 = 895$		
Expt.[5]			$\nu_1 = 3790$	$\nu_2 = 810.3$		

[a] DZP equilibrium geometries are linear, while TZ2P and TZ(2df,2pd) are bent.

[b] CISD+Q Energies are -317.771 652, -317.850 438, and -317.881 655 hartrees, respectively.

Table II. Theoretical predictions of the total energy (in hartrees), dipole moment (in debye), harmonic vibrational frequencies (in cm^{-1}), infrared (IR) intensities (in $km \cdot mol^{-1}$) and zero point vibrational energy (ZPVE) (in $kcal \cdot mol^{-1}$) for $\tilde{X}$ HAlO.

			Vibrational Frequencies/IR Intensities			
Level of Theory	Energy	μ	$\omega_1(a_1)$	$\omega_2(a_1)$	$\omega_3(e_1)$	ZPVE
DZP SCF	-317.330 526	5.400	2143/75	1211/62	492/358	6.201
TZ2P SCF	-317.360 729	5.540	2113/73	1198/73	483/327	6.113
TZ(2df,2pd) SCF	-317.362 558	5.537	2108/73	1198/71	486/328	6.113
DZP CISD[a]	-317.672 215	4.747	2130/66	1138/24	454/258	5.970
TZ2P CISD[a]	-317.745 697	5.032	2078/69	1126/35	445/241	5.855
TZ(2df,2pd) CISD[a]	-317.774 361	5.060	2080/68	1134/36	449/248	5.878
DZP CCSD	-317.702 429	4.532	2088/54	1105/15	429/207	5.791
TZ2P CCSD	-317.780 558	4.815	2025/60	1089/24	420/192	5.652
TZ(2df,2pd) CCSD	-317.811 470	4.847	2026/58	1098/24	424/199	5.678
DZP CCSD(T)	-317.713 115	4.214	2064/54	1065/5	407/170	5.638
TZ2P CCSD(T)	-317.797 058	4.493	2000/62	1048/10	396/157	5.492
TZ(2df,2pd) CCSD(T)	-317.829 670	4.525	2002/59	1056/10	400/163	5.517

[a] CISD+Q Energies are -317.701 586, -317.779 378, and -317.810 418 hartrees, respectively.

Table III. Theoretical predictions of the harmonic vibrational frequencies (in cm^{-1}) for AlOD, the deuterated isotopomer of ground state of AlOH.

	Harmonic Vibrational Frequency		
Level of Theory	$\omega_1(a_1/a')$	$\omega_2(a_1/a')$	$\omega_3(e_1/a')$
DZP SCF	3162	880	113
TZ2P SCF	3134	853	194
TZ(2df,2pd) SCF	3147	866	117
DZP CISD	3036	864	101
TZ2P CISD	3023	832	149
TZ(2df,2pd) CISD	3034	850	91
DZP CCSD	2980	855	77
TZ2P CCSD	2955	817	167
TZ(2df,2pd) CCSD	2967	836	115
DZP CCSD(T)	2962	851	60
TZ2P CCSD(T)	2922	808	166
TZ(2df,2pd) CCSD(T)	2932	827	118
Expt.[7]	$\nu = 2600 \pm 100$	$\nu = 750 \pm 100$	$\nu = 240 \pm 50$
Expt.[5]		$\nu = 795.2$	

Table IV. Theoretical predictions of the harmonic vibrational frequencies (in cm^{-1}) for DAlO, the deuterated isotopomer of ground state of HAlO.

	Harmonic Vibrational Frequency		
Level of Theory	$\omega_1(a_1)$	$\omega_2(a_1)$	$\omega_3(e_1)$
DZP SCF	1566	1186	377
TZ2P SCF	1543	1174	370
TZ(2df,2pd) SCF	1540	1172	372
DZP CISD	1552	1118	347
TZ2P CISD	1514	1106	341
TZ(2df,2pd) CISD	1517	1113	343
DZP CCSD	1521	1085	328
TZ2P CCSD	1475	1070	321
TZ(2df,2pd) CCSD	1476	1077	325
DZP CCSD(T)	1503	1046	312
TZ2P CCSD(T)	1456	1030	303
TZ(2df,2pd) CCSD(T)	1458	1038	306

Table V. Theoretical predictions of the total energy (in hartrees), dipole moment (in debye), harmonic vibrational frequencies (in cm^{-1}), and zero point vibrational energy (ZPVE) (in kcal/mole) for the C_s-symmetry transition state connecting $\tilde{X}$ AlOH and $\tilde{X}$ HAlO.

			Harmonic Vibrational Frequency			
Level of Theory	Energy	μ	$\omega_1(a')$	$\omega_2(a')$	$\omega_3(a'')$	ZPVE
DZP SCF	-317.238 726	4.103	1898	1047	1262*i*	4.210
TZ2P SCF	-317.267 891	4.259	1882	1058	1273*i*	4.203
TZ(2df,2pd) SCF	-317.269 514	4.261	1881	1059	1280*i*	4.202
DZP CISD[a]	-317.596 379	3.954	1881	1027	1097*i*	4.157
TZ2P CISD[a]	-317.668 580	4.156	1853	1028	1095*i*	4.118
TZ(2df,2pd) CISD[a]	-317.695 967	4.200	1864	1039	1119*i*	4.150
DZP CCSD	-317.638 088	3.469	1812	932	979*i*	3.922
TZ2P CCSD	-317.714 921	3.682	1779	934	964*i*	3.877
TZ(2df,2pd) CCSD	-317.744 669	3.721	1791	946	983*i*	3.912
DZP CCSD(T)	-317.653 549	3.315	1779	892	953*i*	3.818
TZ2P CCSD(T)	-317.736 928	3.533	1742	896	932*i*	3.772
TZ(2df,2pd) CCSD(T)	-317.768 556	3.573	1755	909	945*i*	3.808

[a] CISD+Q Energies are -317.636 829, -317.713 007, and -317.742 528 hartrees, respectively.

Table VI. Relative Energies[a] (in kcal/mole) for the ground HAlO-AlOH potential energy hypersurface.

Level of Theory	$\tilde{X}$ AlOH	C_s-symmetry transition state	$\tilde{X}$ HAlO	Barrier Height
DZP SCF	0.00	112.33 (108.64)	54.72 (53.02)	57.60 (55.61)
TZ2P SCF	0.00	110.88 (107.33)	52.63 (50.98)	58.26 (56.35)
TZ(2df,2pd) SCF	0.00	111.71 (108.27)	53.33 (51.79)	58.39 (56.47)
DZP CISD	0.00	93.83 (90.39)	46.24 (44.62)	47.59 (45.77)
TZ2P CISD	0.00	94.85 (91.54)	46.45 (44.89)	48.39 (46.65)
TZ(2df,2pd) CISD	0.00	95.92 (92.72)	46.73 (45.26)	49.19 (47.46)
DZP CISD+Q	0.00	84.60 (81.17)	43.97 (42.35)	40.64 (38.82)
TZ2P CISD+Q	0.00	86.24 (82.94)	44.59 (43.03)	41.65 (39.91)
TZ(2df,2pd) CISD+Q	0.00	87.30 (84.10)	44.70 (43.22)	42.60 (40.87)
DZP CCSD	0.00	85.18 (81.73)	44.80 (43.22)	40.37 (38.51)
TZ2P CCSD	0.00	86.65 (83.22)	45.46 (43.81)	41.19 (39.41)
TZ(2df,2pd) CCSD	0.00	87.48 (84.15)	45.56 (43.99)	41.92 (40.15)
DZP CCSD(T)	0.00	79.33 (75.88)	41.95 (40.32)	37.38 (35.56)
TZ2P CCSD(T)	0.00	79.84 (76.39)	42.11 (40.38)	37.73 (36.01)
TZ(2df,2pd) CCSD(T)	0.00	80.52 (77.16)	42.17 (40.52)	38.35 (36.64)

[a] Numbers in parentheses include zero point vibrational energy corrections. CISD+Q energies were determined at the CISD optimized geometries and corrected for ZPVE using CISD harmonic vibrational frequencies with the same basis set.

Chapter IV

Oxirene: To Be or Not to Be?[1]

---

[1] G. Vacek, J. M. Galbraith, Y. Yamaguchi, H. F. Schaefer, R. H. Nobes, A. P. Scott and L. Radom *J. Phys. Chem.* **98**, 8660 (1994).

The C_{2v}–symmetry structure of oxirene has been examined using *ab initio* molecular orbital calculations with large basis sets and a variety of methods of including electron correlation. Different qualitative conclusions regarding the nature of oxirene are reached depending on the choice of basis set and method of electron correlation incorporation. With certain combinations of basis set and theoretical method, the symmetric oxirene structure is found to be a saddle point on the potential energy surface, while for other combinations oxirene is a local minimum. Inclusion of triple excitations in the correlation treatment has a large effect, tending to make the curvature of the surface corresponding to a ring-opening distortion of the C_{2v}–symmetry structure less positive (or more negative). This is counterbalanced by a basis set effect, with inclusion of *f* functions making the curvature more positive. At our highest level of theory, CCSD(T) with basis sets of triple-zeta quality and including multiple *d* shells and an *f* shell on C and O and multiple *p* shells and a *d* shell on H, oxirene is a genuine minimum under harmonic vibrational analysis, with a ring-opening frequency of 139–163 cm^{-1}.

Introduction

The decomposition–rearrangement of diazoketones and diazoesters to form ketenes and nitrogen, the Wolff rearrangement (1), was first documented in 1902.[1]

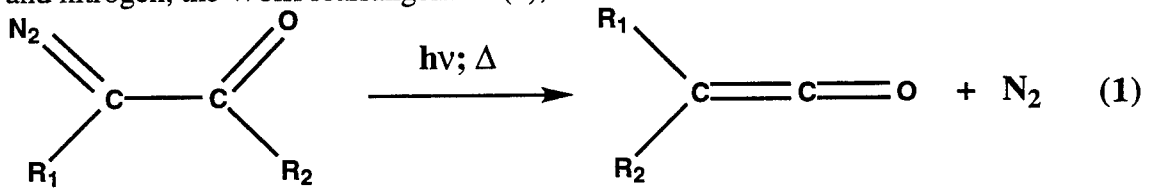

(1)

Although almost a century has passed, the mechanism of the Wolff rearrangement is still in doubt. Numerous possibilities for the mechanism have been proposed, but to date no consensus among chemists has been reached. Meier and Zeller[2] have reviewed the progress made in determining the Wolff rearrangement mechanism, including the possible roles of both free and complexed carbenes, 1,3-dipoles, 1,3-diradicals and oxirenes as intermediates or transition structures. Wolff himself believed that reaction (1) involved ketocarbenes as intermediates. More recently, the participation of symmetric intermediates,

particularly oxirenes, has been proposed and supported by results from isotopic-labeling experiments,[3,4] despite the fact that earlier experimental studies failed to lend support for their existence.[5]

The history of the study of oxirenes, and to some extent ketocarbenes, is well documented in Lewars's 1983 review.[6] At that time, experimental evidence only supported the existence of oxirenes as short-lived intermediates in photochemical and thermal Wolff rearrangements,[3,4] in the peroxyacid oxidations of acetylenes[7] and in ketene photolysis reactions.[8] Since then, evidence has been presented for the observation of a substituted oxirene by laser flash photolysis during a Wolff rearrangement[9] and for the detection by FT-IR spectroscopy of dimethyloxirene, isolated in rare-gas matrices during the photolysis of 3-diazo-2-butanone.[10]

Several experimental attempts have been made to isolate the parent oxirene molecule in the gas phase. Most recently, Hop, Holmes and Terlouw[11] have tried to produce oxirene by the creation and subsequent vertical neutralization of oxirene radical cation, which had been predicted theoretically to be stable.[12] This attempt was unfortunately unsuccessful. Thus, no firm conclusion as to whether unsubstituted oxirenes are true minima on the potential energy surface (PES) or whether they are merely transition structures has yet been reached. Hope for the isolation of oxirene might be taken from the direct observation of the short-lived $\tilde{X}\ ^1A_1$ vinylidene species, which was (albeit with much controversy) predicted to exist with *ab initio* theory[13] and observed by Lineberger's group with negative ion photoelectron spectroscopy.[14] Similar success by similar means was achieved for the $\tilde{X}\ ^1A'$ state of monofluorovinylidene which has an isomerization barrier height of only 2 kcal mol^{-1}.[15,16] Unfortunately, oxirene has no stable anion and so negative ion photoelectron spectroscopy will not be a viable technique for observing neutral oxirene.

Numerous theoretical investigations, both semiempirical[17,18] and *ab initio*,[19–25] have been undertaken on the PES that includes ketene, formylmethylene and oxirene.

MINDO/3 and NDDO calculations[18] find oxirene to be more stable than formylmethylene by about 20 kcal mol^{-1}. *Ab initio* results at the Hartree-Fock level,[19,22–24] on the other hand, show formylmethylene to be more stable than oxirene by 12–17 kcal mol^{-1}. When electron correlation is included through single-point calculations on the Hartree-Fock optimized structures,[23,24] formylmethylene is still favored but the energy difference is reduced to 1–8 kcal mol^{-1}. Moreover, such calculations have suggested that singlet formylmethylene can collapse without a barrier to ketene, the Hartree-Fock transition structure for rearrangement lying lower in energy on the correlated surface than formylmethylene itself.[23,24] We note that, in the thermolysis of diazoketones, the participation of oxirene appears to be small at low temperatures where ketocarbenes are most important but increases with increasing temperature.[4] This implies that ketocarbenes are energetically more stable than oxirenes. This agrees with the *ab initio* energy differences but casts some doubt on the conclusion regarding the stability of formylmethylene reached on the basis of single-point correlated calculations.[23,24]

Ketocarbenes have been isolated in low-temperature matrices.[26] These ketocarbenes were triplet ground states, however, that should not contribute to the Wolff rearrangement which is considered to occur on the singlet surface.[27] Nevertheless, the possibility of singlet–triplet crossing cannot be discarded entirely. The interested reader is referred to an MCSCF study by Novoa, McDouall and Robb for a discussion of this possibility.[28]

Those *ab initio* studies[19–24] which have considered the barrier to ring opening for oxirene have all concluded that the barrier is less than 7.3 kcal mol^{-1}. The most reliable figure is perhaps that of 2 kcal mol^{-1} as determined by Tanaka and Yoshimine by using a reaction coordinate approach.[23] The existence of a barrier at low levels of theory suggests that oxirene should be a minimum, but a more rigorous test lies in vibrational analyses at higher levels of theory. Bouma *et al.*[24] determined that at the HF/3-21G level of theory the C_{2v}–symmetry form of oxirene is a minimum with a ring-opening frequency of 524 cm^{-1}.

More recently Vacek, Colegrove and Schaefer[25] found a decrease (from 524 to 445 cm^{-1}) in the ring-deformation (b_2) vibrational frequency when the basis set is improved moderately (to DZP). The Vacek paper[25] also shows this particular frequency decreasing further (from 445 to 262 cm^{-1}) with inclusion of electron correlation. Although at their highest level of theory (CCSD/DZP) they still conclude that oxirene is a minimum, Vacek *et al.*[25] were not confident that the effects of still larger basis sets and improved treatments of electron correlation would not cause this particular frequency to become imaginary.

Clearly, there are many questions that remain unanswered concerning oxirene and related species that would benefit from a high level *ab initio* determination of the entire oxirene → ketene potential energy hypersurface, and from calculations on related larger homologues. These include the issue of substitution effects on the stability of oxirenes,[29] an understanding of the kinetics of reactions on the C_2H_2O PES[30,31] and further probing of the mechanism for the Wolff rearrangement.[32] In the present paper, we address the particular aspect of whether or not high level *ab initio* calculations indicate oxirene to be a true minimum on the surface.

Theoretical Methods

The C_{2v}–symmetry structure of oxirene was studied with a variety of basis sets and methods of electron correlation. Calculations were carried out using the Gaussian 92/DFT[33] and ACES II[34] programs (at the Australian National University, ANU) and the PSI program (at the Center for Computational Quantum Chemistry, CCQC).[35]

Calculations at the ANU employed the standard 6-31G(*d*), 6-31G(*d,p*) and 6-311G(*d,p*) basis sets[36] and the Dunning correlation-consistent basis, cc-pVTZ.[37] Additional polarization functions and diffuse functions were added to the 6-31G(*d,p*) and 6-311G(*d,p*) basis sets to form the 6-31G(*df,p*), 6-311G(*df,p*) and 6-311+G(*2df,p*) sets.[38,39] Basis sets formed from 6-31G employed sets of six Cartesian *d*-like and ten Cartesian *f*-like polarization functions while those based on 6-311G and cc-pVTZ

employed five pure *d* and seven pure *f* polarization functions, i.e. spherical harmonics.

The DZP basis used in the calculations performed at the CCQC was derived from the standard DZ basis by augmenting with a set of *d*-like functions on the heavy atoms and a set of *p* functions on hydrogen.[38,40] The DZP++ set was constructed by adding diffuse *s* and *p* functions to the DZP basis.[41,42] The TZ2P basis was constructed from the standard TZ basis by the addition of two sets of polarization functions on each atom.[38,43] This basis was further enhanced by the addition of *f*-like polarization functions on the heavy atoms and a set of *d*-like functions on hydrogen,[38,44] leading to the basis referred to as TZ2P(*f,d*) in the text. Yet another basis, TZ2P++, was formed by the addition of diffuse functions to all atoms in the TZ2P set.[41,45] The QZ3P(*f,d*) basis was constructed by the addition of higher angular momentum functions to a standard QZ basis.[38,46] All the CCQC basis sets employed sets of six Cartesian *d*-like and ten Cartesian *f*-like polarization functions.

The molecular structure of oxirene was fully optimized using analytic gradient techniques for restricted Hartree–Fock (RHF),[47] two-configuration SCF (TCSCF),[48] Møller–Plesset perturbation theory (MP*n*)[49–51], configuration interaction (CI),[52,53] coupled-cluster (CC)[54,55] and quadratic configuration interaction (QCI)[56,57] wavefunctions. Density functional calculations were also performed using the local SVWN functional, [58] the gradient-corrected BLYP functional [58,59] and the hybrid Becke3LYP functional.[60] In all cases, the default geometry optimization criteria were employed. [61] For the iterative methods, all single and double excitations (SD) from the SCF reference configuration were included (CISD, CCSD and QCISD). For the coupled-cluster and quadratic configuration methods, the effects of connected triple excitations were included perturbatively [CCSD(T), QCISD(T)].[55,57] In most of the calculations performed at the ANU, all orbitals were correlated (full, abbreviated fu), whereas in the CCQC calculations only the valence electrons were explicitly correlated, i.e. the three lowest-lying MOs (C and O 1s-like) were held doubly occupied (frozen core, abbreviated fc).

For the TCSCF wavefunctions, the second configuration was a double excitation from the highest occupied MO ($2b_1$) to the lowest unoccupied MO ($1a_2$). This is a $\pi \rightarrow \pi^*$ excitation.

The RHF, density functional and MP2 quadratic force constants were evaluated via analytic second derivative procedures.[62–66] The method of finite central differences of the analytically derived gradients was utilized to evaluate the quadratic force constants for the remaining wavefunctions used in this study.

Results and Discussion

Structural Predictions

Total energies and structural predictions are shown in Table I. Perhaps the most interesting feature is the relative insensitivity of the geometrical parameters to basis set improvements for a given theoretical method. For example, with the RHF method, the C–O bond length falls within a range of 0.01 Å across the entire set of bases. This contrasts with the large change seen in going from the smaller basis set 4-31G results (r_{CO} = 1.552 Å) of Tanaka and Yoshimine to their DZ + P results (r_{CO} = 1.465 Å), where there is a change of 0.09 Å.[23] Clearly the first set of polarization functions is very important. On the other hand, increasing the size of the *sp* part of the basis (from a double to a triple split of the valence functions or by adding a set of diffuse functions) has very little effect on the calculated geometry. However, the addition of *f*-like polarization functions does have a significant effect, especially on the C–O bond length (decreasing this length by 0.010–0.015 Å for the conventional correlated methods). It is somewhat reassuring to see the geometrical results converge so quickly with basis set. Unfortunately, as discussed below, the harmonic vibrational frequencies are not so convergent with respect to increase in basis set size.

The changes in geometrical parameters with increasing sophistication of theoretical method are somewhat greater than with basis set. However, the trends observed (namely

an increase in bond lengths as one improves the electron correlation scheme [67,68]) are typical for C–O, C–C and C–H bond distances. For the correlated methods, results with all orbitals included (fu) are very close to those using the frozen-core approach (fc) in the few cases for which direct comparisons are possible. The inclusion of triple excitations in the correlation treatment [MP4SDQ → MP4, QCISD → QCISD(T), CCSD → CCSD(T)] has a relatively large effect, tending to increase the lengths of the C–C and C–O bonds. Note also the large fluctuations in the Møller–Plesset series, with a change of 0.021 Å in the C–O length in going from MP3 to MP4, and the wide range of values for the C–O length from the density functional approaches.

Despite the relatively large changes in the C–O lengths, it appears that the predictions of geometrical structure are converging towards a single set of values with electron correlation. The largest part of the change in geometry occurs between the SCF and either the MP2 or the CISD methods of electron correlation. More sophisticated inclusion of electron correlation has a much smaller effect.

Frequency Predictions

Predictions of the harmonic vibrational frequencies appear in Table II. Of particular interest is the ring-deformation normal vibrational mode. *It can be seen that the nature of the oxirene stationary point changes depending on choice of basis set and theoretical procedure*! If one were to use only SCF calculations, the clear conclusion would be that oxirene is a minimum on the surface. Conversely, all of the density functional based approaches indicate that oxirene is a saddle point. For the conventional correlated procedures, one sees a mixture of real and imaginary values for the ring deformation vibrational mode.

We note initially that the effect of freezing the core in the correlated calculations is very small. For example, the mean absolute difference between the QCISD-fc/6-31G(*d*) and QCISD-fu/6-31G(*d*) frequencies is just 3 cm^{-1}, with a largest difference of 13 cm^{-1}.

The drop in the ring-opening harmonic vibrational frequency from RHF/DZP (445 cm^{-1}) to CISD/DZP (338 cm^{-1}) to CCSD/DZP (262 cm^{-1}) has already been noted by Vacek *et al.*[25] Inclusion of triple excitations in the correlation treatment has a large effect, further flattening the surface at the C_{2v}–symmetry stationary point. For example, for the DZP basis set, there is another drop (to 119 cm^{-1}) when going to the CCSD(T) method of electron correlation. Furthermore, when making rather typical basis set improvements [such as from DZP to TZ2P or 6-31G(*d,p*) to 6-311G(*d,p*)], we again see a lowering of this vibrational frequency. This effect is somewhat additive and as a result it can be seen that at the CCSD(T) level with large *spd* basis sets the surface actually has negative curvature, i.e. oxirene is a saddle point at these levels of theory!

However *all* other basis set improvements seem to stabilize oxirene with respect to ring deformation. The addition of diffuse functions to the DZP and TZ2P bases slightly decreases the C–O bond length and stabilizes the mode in question by 12 and 6 cm^{-1}, respectively, on the RHF surfaces and by 56 and 72 cm^{-1} on the CCSD(T) surfaces. Note also that, although the initial valence and polarization improvement from DZP to TZ2P was destabilizing, an additional improvement from TZ2P(*f,d*) to QZ3P(*f,d*) is stabilizing, at least on the RHF surface.

The stabilization of oxirene by higher angular momentum functions is even greater than that by diffuse functions. For example, with the CCSD(T) method, the addition of an *f* shell to the 6-311G(*d,p*) basis or *f* (on C and O) and *d* (on H) shells to the TZ2P basis has a large effect, restoring positive curvature to the potential surface. With our best theoretical levels, CCSD(T)-fc/TZ2P(*f,d*) and CCSD(T)-fu/cc-pVTZ, oxirene is a local minimum on the potential surface with ring-opening frequencies of 163 and 139 cm^{-1}, respectively.

The poor performance of Møller–Plesset perturbation theory for this problem should be noted. One can see rather large fluctuations in the b_2 vibrational frequency along the series RHF $\rightarrow$ MP2 $\rightarrow$ MP3 $\rightarrow$ MP4 (459 $\rightarrow$ 135 $\rightarrow$ 400 $\rightarrow$ 207 *i* cm^{-1}) for the

6-311G(*df,p*) basis. The importance of a balanced treatment of triple substitutions is also nicely illustrated by results with the 6-311G(*df,p*) basis set. MP4 without the triples (MP4SDQ) has a ring-opening frequency of 227 cm^{-1}. This changes dramatically to 207 *i* cm^{-1} when triples are included (MP4). MP4 is, however, known[69,70] to overestimate the importance of the triple substitutions. A more complete treatment of the triples is provided by QCISD(T) for which the ring-opening frequency becomes real (82 cm^{-1}). CCSD(T) results in a further improvement in the treatment of the triple effects,[70] and at the CCSD(T)/6-311G(*df,p*) level the b_2 frequency increases to 137 cm^{-1}. The effect of the inclusion of quadruple excitations[71] on the geometry and the ring-opening frequency of oxirene would certainly be of interest!

A brief aside should be made concerning the possible importance of a multireference wavefunction. For all three CISD wavefunctions constructed in this study, the coefficient of the reference configuration is 0.94. The coefficients for the second most important configuration (a double excitation from the $2b_1$ π_{CC}-bonding MO to the $1a_2$ π^*_{CC}-antibonding MO) are -0.06, -0.05 and -0.04 for increasing-sized basis sets. Such contributions from the second configuration imply that single-reference CISD may not be entirely suitable. However, analysis of the coupled-cluster wavefunctions reveal T_1 diagnostic values of 0.014 for all cases. This is less than the suggested threshold of 0.02,[72] implying that most of the dynamical correlation energy is being recovered by the coupled-cluster wavefunctions. Thus while CISD results are suggested to be insufficient, coupled-cluster wavefunctions should be adequate to resolve the problem without resorting to multireference techniques. This last conclusion, of course, only pertains to the oxirene stationary point and does not necessarily apply to the entire isomerization hypersurface.

Conclusion

The present study has examined the C_{2v}–symmetry structure of oxirene with a variety of basis sets and theoretical procedures. The results at the various levels show

qualitative differences, specifically with regard to the nature of the stationary point. Density functional methods, fourth-order Møller–Plesset perturbation theory and CCSD(T) methods with large *spd* basis sets all show the symmetric structure to be a transition structure along the ring-opening normal coordinate, while other methods show it to be a true minimum. At our highest level of theory, CCSD(T) with basis sets of triple-zeta quality and including multiple *d* shells and an *f* shell on C and O and multiple *p* shells and a *d* shell on H, oxirene is a true minimum with a ring-opening frequency of 139–163 cm^{-1}.

The large basis set CCSD(T) calculations may prove prohibitively costly for studying the low-symmetry structures in the oxirene → ketene isomerization. A compromise in terms of computational efficiency and accuracy may be provided by the CCSD(T)/6-311G(*df,p*) level of theory, which predicts a geometry and a ring-opening frequency satisfactorily close to those given by the CCSD(T)/cc-pVTZ and CCSD(T)/TZ2P(*f,d*) methods.

Acknowledgements

This research was supported by the U.S. Department of Energy, Office of Basic Energy Sciences, Grant No. DE-FG09-87ER13811. GV is supported under a U.S. Department of Defense Graduate Fellowship. GV, JMG, YY and HFS would like to thank Dan Gezelter and William H. Miller for interesting discussions. APS, RHN and LR thank the Australian National University Supercomputer Facility for a generous allocation of time on the Fujitsu VP2200.

References

1. L. Wolff, *Justus Liebigs Ann. Chem.* **325**, 129 (1902); **394**, 23 (1912).

2. H. Meier and K.-P. Zeller, *Angew. Chem. Int. Ed. Engl.* **14**, 32 (1975).

3. I. G. Csizmadia, J. Font and O. P. Strausz, *J. Am. Chem. Soc.* **90**, 7360 (1968); D. E. Thornton, R. K. Gosavi and O. P. Strausz, *J. Am. Chem. Soc.* **92**,

1768 (1970).

4. S. A. Matlin and P. G. Sammes, *J. Chem. Soc. Chem. Commun.* 11 (1972); *J. Chem. Soc. Perkin Trans.* **1**, 2623 (1972); 2851 (1973).

5. C. Huggett, R. T. Arnold and T. I. Taylor, *J. Am. Chem. Soc.* **64**, 3043 (1942); V. Franzen, Annalen. **614**, 31 (1958).

6. E. G. Lewars, *Chem. Rev.* **83**, 519 (1983).

7. R. N. McDonald and P. A. Schwab, *J. Am. Chem. Soc.* **86**, 4866 (1964); J. K. Stille and D. D. Whitehurst, *J. Am. Chem. Soc.* **86**, 4871 (1964).

8. R. L. Russell and F. S. Rowland, *J. Am. Chem. Soc.* **92**, 7508 (1970).

9. K. Tanigaki and T. W. Ebbesen, *J. Am. Chem. Soc.* **109**, 5883 (1987).

10. F. Debu, M. Monnier, P. Verlaque, G. Davidovics, J. Pourcin, H. Bodot and J.-P. Aycard, *C. R. Acad. Sci. Paris Ser. 2* **303**, 897 (1986); C. Bachmann, T. Y. N'Guessan, F. Debu, M. Monnier, J. Pourcin, J.-P. Aycard and H. Bodot, *J. Am. Chem. Soc.* **112**, 7488 (1990).

11. C. E. C. A. Hop, J. L. Holmes and J. K. Terlouw, *J. Am. Chem. Soc.* **111**, 441 (1989).

12. W. J. Bouma, P. M. W. Gill, and L. Radom, *Org. Mass Spectrom.* **19**, 610 (1984).

13. C. E. Dykstra and H. F. Schaefer, *J. Am. Chem. Soc.* **100**, 1378 (1978); M. M. Gallo, T. P. Hamilton and H. F. Schaefer, *J. Am. Chem. Soc.* **112**, 8714 (1990); B. J. Smith, R. Smernik and L. Radom, *Chem. Phys. Lett.* **188**, 589 (1992).

14. K. M. Ervin, J. Ho and W. C. Lineberger, *J. Chem. Phys.* **91**, 5974 (1989).

15. M. K. Gilles, W. C. Lineberger and K. M. Ervin, *J. Am. Chem. Soc.* **115**, 1031 (1993).

16. B. J. DeLeeuw, J. T. Fermann, Y. Xie and H. F. Schaefer, *J. Am. Chem. Soc.* **115**, 1039 (1993).

17. I. G. Csizmadia, H. E. Gunning, R. K. Gosavi and O. P. Strausz, *J. Am. Chem. Soc.* **95**, 133 (1973).

18. M. J. S. Dewar and C. A. Ramsden, *J. Chem. Soc. Chem. Commun.* 688 (1973).

19. O. P. Strausz, R. K. Gosavi and H. E. Gunning, *J. Chem. Phys.* **67**, 3057 (1977); *Chem. Phys. Lett.* **54**, 510 (1978).

20. C. E. Dykstra, *J. Chem. Phys.* **68**, 4244 (1978).

21. N. C. Baird and K. F. Taylor, *J. Am. Chem. Soc.* **100**, 1333 (1978).

22. O. P. Strausz, R. K. Gosavi, A. S. Denes and I. G. Csizmadia, *J. Am. Chem. Soc.* **98**, 4784 (1976).

23. K. Tanaka and M. Yoshimine, *J. Am. Chem. Soc.* **102**, 7655 (1980).

24. W. J. Bouma, R. H. Nobes, L. Radom and C. E. Woodward, *J. Org. Chem.* **47**, 1869 (1982).

25. G. Vacek, B. T. Colegrove and H. F. Schaefer, *Chem. Phys. Lett.* **177**, 468 (1991).

26. A. M. Trozzolo *Acc. Chem. Res.* **1**, 329 (1968); R. S. Hutton, M. L. Manion, H. D. Roth and E. Wasserman, *J. Am. Chem. Soc.* **96**, 4680 (1974); R. S. Hutton and H. D. Roth, *J. Am. Chem. Soc.* **100**, 4324 (1978).

27. A. Padwa and R. Layton, *Tetrahedron Lett.* 2167 (1965); M. Jones and W. Ando, *J. Am. Chem. Soc.* **90**, 2200 (1968); T. DoMinh and O. P. Strausz, *J. Am. Chem. Soc.* **92**, 1766 (1970).

28. J. J. Novoa, J. J. W. McDouall and M. A. Robb, *J. Chem. Soc. Faraday Trans. 2* **83**, 1629 (1987); see also: R. K. Gosavi, M. Torres and O. P. Strausz, *Can. J. Chem.* **69**, 1630 (1991).

29. J. E. Fowler, J. M. Galbraith, G. Vacek and H. F. Schaefer, *J. Am. Chem. Soc.* **116**, 9311 (1994).

30. E. R. Lovejoy, S. K. Kim, R. A. Alvarez and C. B. Moore, *J. Chem. Phys.* **95**, 4081 (1991); E. R. Lovejoy, S. K. Kim and C. B. Moore, *Science* **256**,

1541 (1992); E. R. Lovejoy and C. B. Moore, *J. Chem. Phys.* **98**, 7846 (1993).

31. D. Gezelter, W. H. Miller, G. Vacek and H. F. Schaefer, in progress.

32. A. P. Scott, R. H. Nobes, H. F. Schaefer and L. Radom, *J. Am. Chem. Soc.* **116**, 10165 (1994).

33. Gaussian 92/DFT, Revision F.3, M. J. Frisch, G. W. Trucks, H. B. Schlegel, P. M. W. Gill, B. G. Johnson, M. W. Wong, J. B. Foresman, M. A. Robb, M. Head-Gordon, E. S. Replogle, R. Gomperts, J. L. Andres, K. Raghavachari, J. S. Binkley, G. Gonzales, R. L. Martin, D. J. Fox, D. J. DeFrees, J. Baker, J. J. P. Stewart and J. A. Pople, Gaussian, Inc., Pittsburgh, PA, 1993.

34. ACES II, Version 0.2, J. F. Stanton, J. Gauss, J. D. Watts, W. J. Lauderdale and R. J. Bartlett, Quantum Theory Project, University of Florida, 1992; J. F. Stanton, J. Gauss, J. D. Watts, W. J. Lauderdale and R. J. Bartlett, *Int. J. Quantum. Chem.* **S26**, 879 (1992).

35. PSI2.0.8; C. L. Janssen, E. T. Seidl, G. E. Scuseria, T. P. Hamilton, Y. Yamaguchi, R. B. Remington, Y. Xie, G. Vacek, C. D. Sherrill, T. D. Crawford, J. T. Fermann, W. D. Allen, B. R. Brooks, G. B. Fitzgerald, D. J. Fox, J. F. Gaw, N. C. Handy, W. D. Laidig, T. J. Lee, R. M. Pitzer, J. E. Rice, P. Saxe, A. C. Scheiner and H. F. Schaefer, PSITECH, Inc., Watkinsville, GA, 30677, U. S. A., 1994.

36. P. C. Hariharan and J. A. Pople, *Theor. Chim. Acta*, **28**, 213 (1973); R. Krishnan, J. S. Binkley, R. Seeger and J. A. Pople, *J. Chem. Phys.* **72**, 650 (1980).

37. (10*s*5*p*2d1*f*)/[4*s*3*p*2*d*1*f*]: T. H. Dunning, Jr. *J. Chem. Phys.* **90**, 1007 (1989).

38. M. J. Frisch, J. A. Pople and J. S. Binkley, *J. Chem. Phys.* **80**, 3265 (1984).

39. α_f(C) = 0.8 and α_f(O) = 1.4.

40. (9*s*5*p*)/[4*s*2*p*], α_d(C) = 0.75, α_d(O) = 0.85: (4*s*)/[2*s*], α_p(H) = 0.75: T. H. Dunning, *J. Chem. Phys.* **53**, 2823 (1970).

41. T. J. Lee and H. F. Schaefer, *J. Chem. Phys.* **83**, 1784 (1985).

42. α_s(C) = 0.031069, α_p(C) = 0.036290, α_s(O) = 0.057122, α_p(O) = 0.065082 and α_s(H) = 0.044150.

43. (10*s*6*p*)/[5*s*3*p*], α_d(C) = 1.50, 0.375, α_d(O) = 1.70, 0.425: (5*s*)/[3*s*], α_p(H) = 1.50, 0.375: T. H. Dunning *J. Chem. Phys.* **55**, 716 (1971).

44. α_f(C) = 0.8, α_f(O) = 1.4 and α_d(H) = 1.0.

45. α_s(C) = 0.048116, α_p(C) = 0.033886, α_s(O) = 0.089929, α_p(O) = 0.058397 and α_s(H) = 0.030158.

46. (11*s*7*p*)/[6*s*4*p*], α_d(C) = 3.0, 0.75, 0.1875, α_d(O) = 3.4, 0.85, 0.2125 and α_p(H) = 3.0, 0.75, 0.1875: F. B. Van Duijneveldt, *IBM Report 945*, Tables A2 and A34.

47. P. Pulay, *Adv. Chem. Phys.* **69**, 241 (1987).

48. Y. Osamura, Y. Yamaguchi and H. F. Schaefer, *J. Chem. Phys.* **77**, 383 (1982); Y. Yamaguchi, Y. Osamura and H. F. Schaefer, *J. Am. Chem. Soc.* **105**, 7506 (1983).

49. J. A. Pople, R. Krishnan, H. B. Schlegel and J. S. Binkley, *Int. J. Quantum Chem.* **S13,** 225 (1979); M. J. Frisch, M. Head-Gordon and J. A. Pople, *Chem. Phys. Lett.* **166**, 275 (1990); 281 (1990).

50. G. Fitzgerald, R. Harrison, W. D. Laidig and R. J. Bartlett, *J. Chem. Phys.* **82,** 4375 (1985).

51. J. Gauss and D. Cremer, *Chem. Phys. Lett.* **138**, 131 (1987); **153**, 303 (1988).

52. B. R. Brooks, W. D. Laidig, P. Saxe, J. D. Goddard, Y. Yamaguchi and H. F. Schaefer, *J. Chem. Phys.* **72**, 4652 (1980).

53. J. E. Rice, R. D. Amos, N. C. Handy, T. J. Lee and H. F. Schaefer, *J. Chem.*

Phys. **85**, 963 (1986).

54. A. C. Scheiner, G. E. Scuseria, J. E. Rice, T. J. Lee and H. F. Schaefer, *J. Chem. Phys.* **87**, 5361 (1987); G. E. Scuseria, C. L. Janssen and H. F. Schaefer, *J. Chem. Phys.* **89**, 7383 (1988); J. Gauss, J. F. Stanton and R. J. Bartlett, *J. Chem. Phys.* **95**, 2623 (1991); A. P. Rendell and T. J. Lee, *J. Chem. Phys.* **94**, 6219 (1991).

55. G. E. Scuseria, *J. Chem. Phys.* **94**, 442 (1991); E. A. Salter, G. W. Trucks and R. J. Bartlett, *J. Chem. Phys.* **90**, 1752 (1989); T. J. Lee and A. P. Rendell, *J. Chem. Phys.* **94**, 6229 (1991).

56. J. Gauss and D. Cremer, *Chem. Phys. Lett.* **150**, 280 (1988).

57. J. Gauss and D. Cremer, *Chem. Phys. Lett.* **163**, 549 (1989).

58. B. G. Johnson, P. M. W. Gill and J. A. Pople, *J. Chem. Phys.* **97**, 7846 (1992); **98**, 5612 (1993).

59. P. M. W. Gill, B. G. Johnson, J. A. Pople and M. J. Frisch, *Chem. Phys. Lett.* **197**, 499 (1992).

60. A. D. Becke, to be published.

61. For the DFT calculations the default SG-1 grid was used: P. M. W. Gill, B. G. Johnson and J. A. Pople, *Chem. Phys. Lett.* **209**, 506 (1993).

62. P. Saxe, D. J. Fox, H. F. Schaefer and N. C. Handy, *J. Chem. Phys.* **77**, 5584 (1982).

63. B. G. Johnson and M. J. Frisch, *Chem. Phys. Lett.* **216**, 133 (1993). see also: N. C. Handy, D. J. Tozer, G. J. Laming, C. W. Murray and R. D. Amos, *Israel J. Chem.* **33**, 331 (1993).

64. Y. Osamura, Y. Yamaguchi, P. Saxe, M. A. Vincent and H. F. Schaefer, *Chem. Phys.* **72**, 131 (1982).

65. Y. Osamura, Y. Yamaguchi, P. Saxe, D. J. Fox, M. A. Vincent and H. F. Schaefer, *J. Mol. Struct.* **103**, 183 (1983) .

66. H. B. Schlegel, J. S. Binkley and J. A. Pople, *J. Chem. Phys.* **80**, 1976 (1984).

67. W. J. Hehre, L. Radom, P. v. R. Schleyer and J. A. Pople, *Ab Initio Molecular Orbital Theory*, (Wiley, New York, 1986).

68. J. R. Thomas, B. J. DeLeeuw, G. Vacek and H. F. Schaefer, *J. Chem. Phys.* **98**, 1336 (1993); J. R. Thomas, B. J. DeLeeuw, G. Vacek, T. D. Crawford, Y. Yamaguchi and H. F. Schaefer, *J. Chem. Phys.* **99**, 403 (1993); B. J. DeLeeuw, J. R. Thomas, G. Vacek, Y. Yamaguchi and H. F. Schaefer, to be published.

69. J. A. Pople, M. Head-Gordon and K. Raghavachari, *Int. J. Quantum Chem.* **S22**, 377 (1988).

70. See for example: Z. He and D. Cremer, *Int. J. Quantum Chem.* **S25**, 43 (1991); Z. He and D. Cremer, *Theor. Chim. Acta.* **85**, 305 (1993).

71. K. Raghavachari, J. A. Pople, E. S. Replogle and M. Head-Gordon, *J. Phys. Chem.* **94**, 5579 (1993).

72. T. J. Lee and P. R. Taylor, *Int. J. Quantum Chem.* **S23**, 199 (1989).

TABLE I. Calculated total energies and molecular structures for the C_{2v}–symmetry structure of oxirene.[a]

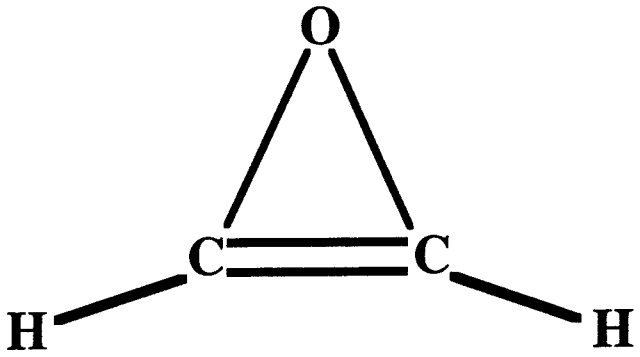

Level of theory[b,c]	Src.[d]	Tot. E.[e]	r(C - O)	r(C = C)	r(C - H)	<CCH
RHF/6-31G(*d*)	ANU	-1.58390	1.467	1.244	1.062	162.8
RHF/DZP	CCQC	-1.61718	1.466	1.251	1.066	162.6
RHF/DZP++	CCQC	-1.62189	1.464	1.251	1.066	162.7
RHF/6-311G(*d,p*)	ANU	-1.62365	1.464	1.243	1.061	162.8
RHF/6-311G(*df,p*)	ANU	-1.63164	1.459	1.241	1.061	162.6
RHF/TZ2P	CCQC	-1.64283	1.465	1.240	1.059	162.2
RHF/TZ2P++	CCQC	-1.64395	1.464	1.240	1.059	162.3
RHF/cc-pVTZ[f]	ANU	-1.64536	1.460	1.240	1.059	162.5
RHF/TZ2P(*f,d*)	CCQC	-1.65069	1.459	1.240	1.059	162.5
RHF/QZ3P(*f,d*)	CCQC	-1.65686	1.457	1.240	1.059	162.5
TCSCF/DZP	CCQC	-1.64882	1.461	1.274	1.065	162.8
TCSCF/TZ2P	CCQC	-1.67329	1.460	1.261	1.058	162.5
SVWN/6-311G(*df,p*)	ANU	-1.69702	1.481	1.265	1.081	161.8
BLYP/6-311G(*d,p*)	ANU	-2.47827	1.530	1.273	1.076	161.7
BLYP/6-311G(*df,p*)	ANU	-2.48410	1.525	1.271	1.077	161.4

BLYP/6-311+G(*2df,p*)	ANU	-2.49660	1.523	1.270	1.077	161.6
Becke3LYP/6-311G(*df,p*)	ANU	-2.51811	1.499	1.261	1.071	161.7
MP2-fc/6-31G(*d*)	ANU	-2.01868	1.512	1.277	1.074	161.9
MP2-fc/6-311G(*d,p*)	ANU	-2.09517	1.504	1.277	1.071	162.2
MP2-fc/6-311G(*df,p*)	ANU	-2.14680	1.492	1.274	1.073	161.9
MP2-fu/6-311G(*df,p*)	ANU	-2.20418	1.489	1.272	1.072	161.8
MP2-fc/6-311+G(2*df,p*)	ANU	-2.18535	1.500	1.271	1.071	162.0
MP2-fu/cc-pVTZ[f]	ANU	-2.23792	1.497	1.268	1.064	161.8
MP3-fu/6-311G(*df,p*)	ANU	-2.21512	1.475	1.266	1.071	161.8
MP4SDQ-fu/6-311G(*df,p*)	ANU	-2.22060	1.482	1.268	1.072	161.9
MP4-fu/6-311G(*df,p*)	ANU	-2.24683	1.496	1.277	1.074	161.9
CISD-fc/DZP	CCQC	-2.02266	1.491	1.272	1.073	162.0
CISD-fc/TZ2P	CCQC	-2.09860	1.488	1.255	1.062	161.5
CISD-fc/TZ2P(*f,d*)	CCQC	-2.14890	1.475	1.253	1.061	162.1
QCISD-fc/6-31G(*d*)	ANU	-2.03619	1.506	1.275	1.075	162.1
QCISD-fu/6-31G(*d*)	ANU	-2.04774	1.504	1.273	1.075	162.2
QCISD-fu/6-311G(*df,p*)	ANU	-2.22152	1.483	1.269	1.072	162.0
QCISD(T)-fc/6-31G(*d*)	ANU	-2.05324	1.514	1.281	1.077	162.0
QCISD(T)-fu/6-31G(*d*)	ANU	-2.06494	1.512	1.280	1.077	161.9
QCISD(T)-fu/6-311G(*df,p*)	ANU	-2.24511	1.490	1.276	1.074	161.9

CCSD-fc/DZP	CCQC	-2.07317	1.506	1.285	1.078	161.8
CCSD-fu/6-311G(*df,p*)	ANU	-2.22005	1.481	1.269	1.072	161.9
CCSD-fc/TZ2P	CCQC	-2.15573	1.505	1.267	1.067	161.3
CCSD(T)-fu/6-31G(*d*)	ANU	-2.06428	1.512	1.279	1.076	161.9
CCSD(T)-fu/6-31G(*d,p*)	ANU	-2.08064	1.510	1.280	1.070	161.6
CCSD(T)-fu/6-31G(*df,p*)	ANU	-2.16296	1.500	1.269	1.071	161.8
CCSD(T)-fc/DZP	CCQC	-2.09085	1.515	1.292	1.080	161.7
CCSD(T)-fc/DZP++	CCQC	-2.10026	1.513	1.291	1.079	161.9
CCSD(T)-fu/6-311G(*d,p*)	ANU	-2.18937	1.504	1.280	1.073	161.9
CCSD(T)-fu/6-311G(*df,p*)	ANU	-2.24439	1.490	1.276	1.074	161.8
CCSD(T)-fc/TZ2P	CCQC	-2.18130	1.518	1.275	1.069	161.2
CCSD(T)-fc/TZ2P++	CCQC	-2.18349	1.517	1.275	1.069	161.2
CCSD(T)-fu/cc-pVTZ[f]	ANU	-2.27586	1.497	1.270	1.065	161.9
CCSD(T)-fc/TZ2P(*f,d*)	CCQC	-2.23948	1.503	1.273	1.069	161.8

[a] Energies in hartrees, bond lengths in angströms, bond angles in degrees.

[b] The notation "fu" (full) indicates that all orbitals were included in the correlation treatment while "fc" (frozen-core) indicates that the core orbitals were held frozen.

[c] Calculations based on the 6-31G or CCQC basis sets used 6*d* and/or 10*f* while calculations based on 6-311G or cc-pVTZ used 5*d* and/or 7*f*.

[d] ANU: Australian National University, Canberra; CCQC: Center for Computational Quantum Chemistry, Athens.

[e] Total energy -150 hartrees.

[f] [4*s*3*p*2*d*1*f*]

TABLE II. Calculated harmonic vibrational frequencies for the C_{2v}–symmetry structure of oxirene.[a]

Level of theory[b,c]	Src[d]	CH stretch (a_1)	CC stretch (a_1)	CO stretch (a_1)	CH rock (a_1)	CH wag (a_2)	CH wag (b_1)	CH stretch (b_2)	CH rock (b_2)	ring deform. (b_2)
RHF/6-31G(*d*)	ANU	3618	2004	1180	998	795	693	3537	1095	440
RHF/DZP	CCQC	3581	1971	1170	994	786	673	3502	1087	445
RHF/DZP++	CCQC	3584	1971	1171	995	789	675	3500	1087	457
RHF/6-311G(*d,p*)	ANU	3576	1978	1167	999	821	692	3492	1096	441
RHF/6-311G(*df,p*)	ANU	3575	1979	1182	1002	826	693	3493	1105	459
RHF/TZ2P	CCQC	3575	1969	1160	982	785	677	3492	1094	416
RHF/TZ2P++	CCQC	3575	1968	1159	982	781	674	3492	1094	422
RHF/cc-pVTZ[e]	ANU	3570	1976	1173	998	823	689	3485	1106	446
RHF/TZ2P(*f,d*)	CCQC	3570	1975	1169	996	833	695	3488	1105	446
RHF/QZ3P(*f,d*)	CCQC	3568	1976	1174	1000	832	692	3487	1111	456
TCSCF/DZP	CCQC	3567	1834	1185	985	176	236 *i*	3506	1081	566
TCSCF/DZP++	CCQC	3563	1834	1173	974	122	242 *i*	3496	1088	531

SVWN/6-311G(*df,p*)	ANU	3320	1810	1084	870	585	478	3243	919	354 *i*
BLYP/6-311G(*d,p*)	ANU	3315	1764	1011	836	558	500	3244	903	394 *i*
BLYP/6-311G(*df,p*)	ANU	3312	1770	1022	840	569	499	3241	914	374 *i*
BLYP/6-311+G(2*df,p*)	ANU	3310	1765	1009	837	604	513	3241	915	310 *i*
Becke3LYP/6-311G(*df,p*)	ANU	3397	1833	1072	889	647	546	3323	966	183 *i*
MP2-fc/6-31G(*d*)	ANU	3458	1800	1107	889	481	467	3390	950	42 *i*
MP2-fc/6-311G(*d,p*)	ANU	3445	1768	1098	894	581	510	3375	955	128 *i*
MP2-fc/6-311G(*df,p*)	ANU	3442	1781	1124	903	556	475	3372	970	129
MP2-fu/6-311G(*df,p*)	ANU	3454	1787	1126	905	573	482	3384	974	135
MP2-fc/6-311+G(2*df,p*)	ANU	3426	1775	1082	884	628	517	3358	958	158
MP2-fu/cc-pVTZ[e]	ANU	3455	1785	1098	895	614	516	3370	972	135
MP3-fu/6-311G(*df,p*)	ANU	3474	1843	1161	931	608	511	3403	999	400
MP4SDQ-fu/6-311G(*df,p*)	ANU	3455	1820	1137	917	583	505	3383	988	227
MP4-fu/6-311G(*df,p*)	ANU	3425	1760	1103	887	509	457	3356	958	207 *i*
CISD-fc/DZP	CCQC	3500	1866	1134	932	652	561	3427	1009	336

CISD-fc/TZ2P	CCQC	3500	1873	1119	924	608	581	3417	1011	310
CISD-fc/TZ2P(*f,d*)	CCQC	3514	1894	1135	946	733	616	3436	1032	364
QCISD-fc/6-31G(*d*)	ANU	3433	1818	1095	889	494	461	3365	948	119
QCISD-fu/6-31G(*d*)	ANU	3435	1821	1097	891	499	474	3366	950	121
QCISD-fu/6-311G(*df,p*)	ANU	3448	1815	1128	913	573	503	3377	985	207
QCISD(T)-fu/6-31G(*d*)	ANU	3409	1777	1079	868	448	389	3342	929	90 *i*
QCISD(T)-fu/6-311G(*df,p*)	ANU	3422	1769	1109	890	499	451	3354	962	82
CCSD-fc/DZP	CCQC	3429	1784	1099	890	552	487	3361	969	263
CCSD-fu/6-311G(*df,p*)	ANU	3450	1821	1136	917	582	506	3379	989	285
CCSD-fc/TZ2P	CCQC	3420	1791	1081	878	517	495	3341	965	228
CCSD(T)-fu/6-31G(*d*)	ANU	3410	1781	1081	870	451	396	3343	931	21
CCSD(T)-fu/6-31G(*d,p*)	ANU	3449	1780	1092	875	448	426	3381	948	48
CCSD(T)-fu/6-31G(*df,p*)	ANU	3435	1788	1105	895	522	493	3368	977	218
CCSD(T)-fc/DZP	CCQC	3405	1739	1076	865	488	439	3339	947	119

CCSD(T)-fc/DZP++	CCQC	3410	1741	1074	865	489	464	3336	945	165
CCSD(T)-fu/6-311G(*d,p*)	ANU	3415	1751	1080	878	518	481	3347	941	122 *i*
CCSD(T)-fu/6-311G(*df,p*)	ANU	3422	1772	1111	892	502	453	3355	964	137
CCSD(T)-fc/TZ2P	CCQC	3392	1739	1055	846	476	418	3314	936	85 *i*
CCSD(T)-fc/TZ2P++	CCQC	3391	1738	1053	846			3313	937	13 *i*
CCSD(T)-fu/cc-pVTZ[e]	ANU	3425	1775	1084	884	567	500	3339	966	139
CCSD(T)-fc/TZ2P(*f,d*)	CCQC	3407	1763	1067	873	591	514	3338	960	163

[a] Harmonic vibrational frequencies in cm^{-1}.

[b] The notation "fu" (full) indicates that all orbitals were included in the correlation treatment while "fc" (frozen-core) indicates that the core orbitals were held frozen.

[c] Calculations based on the 6-31G or CCQC basis sets used 6*d* and/or 10*f* while calculations based on 6-311G or cc-pVTZ used 5*d* and/or 7*f*.

[d] ANU: Australian National University, Canberra; CCQC: Center for Computational Quantum Chemistry, Athens.

[e] [4*s*3*p*2*d*1*f*]

Chapter V: Concluding Remarks

When I started doing theoretical chemistry in the summer of 1990, I thought that the computer would do all the work for me. Here I was only partly right. The computer can solve the equations that I tell it to (within certain limits, of course), as far as handling the integrals and summations and what not. However, it is not as simple as all that.

Firstly, a project needs to be chosen for which theoretical methods can reasonably be expected to add sufficient insight to illuminate the chemical problem. While chemical problems are numerous, not all fit the above standards. For instance, many chemical systems are too large to be accurately studied with current computer resources. Fortunately for those of us in this field, computers are getting "larger" at a very good rate. Projects which were difficult to study on the campus mainframe when I started five years ago can now be handled on a personal computer. Even if the chemical system is small enough, standard methods will have somewhat more difficulty with excited states and weakly bound complexes and certain other systems.

Provided with a suitable chemical system, one faces the second challenge of choosing the best level of theory with which to study the system. Generally the trade-off is between relative accuracy of results and consumption of computer resources. That is, low accuracy with little consumption or higher accuracy at greater expense. To make matters worse, there is no *a priori* way to know how accurate a particular method will be for a particular system. Experience and/or systematic studies on related systems will help by providing guidelines to this choice, but often one must just keep beating the problem with successively bigger theoretical hammers until the desired degree of accuracy is achieved.

The final consideration in computational theoretical chemistry which prevents the computer from completing the research for us is the nature of the input and output data. As with any computation, garbage in means garbage out. A decent chemical understanding of the system of interest is therefor a must to give the correct input. Furthermore, chemical intuition is necessary to sort the output data in some meaningful manner.

So, as I stated, theoretical computational chemistry turns out to not be quite so simple as I had believed prior to starting in the field. However, the fact that it is no so easy is the only thing which keeps it from getting boring (and me from getting replaced by said computer). Besides, I'll take this over longhand calculations on the chalkboard any day.

I will end with some closing remarks about the individual projects that comprise this work.

Within my earshot, acetylene (really all C_2H_2 systems) was referred to as "the little system that could." These systems have been studied by chemists since the dawn of chemistry, and more recently by theoretical chemists since the dawn of theoretical chemistry. Yet there still remain many interesting questions to be answered about these systems, not to mention the many related A_2H_2 systems for which C_2H_2 is a model. Here we have demonstrated that for these systems in order to obtain relative energetic predictions to within an accuracy of 2 kcal/mole, it is necessary to use basis sets with multiple polarization functions as well as higher-angular-momentum polarization functions and include electron correlation from higher than singles and doubles excitations. The isomerization reaction from $\tilde{b}\ ^3B_u$ *trans*-bent to $\tilde{a}\ ^3B_2$ *cis*-bent acetylene is predicted to be exothermic by 8.3 kcal/mole with a barrier height of *only* 4.8 kcal/mole. This may help explain why the *trans* state has yet to be experimentally characterized. Hopefully our definitive theoretical predictions will provide a stimulus for the full experimental characterization of the lowest triplet states of C_2H_2.

All the research in this theoretical work has been completed with the thought in mind that it would influence and aid not only other theoretical chemists but also

experimental chemists. Thus it is all the more gratifying that the study of AlOH-HAlO helped experimentalists whom I know personally. Our predictions compared sufficiently well to their experimental results so as to confirm the assignments which they determined. Not all projects work out this fruitfully.

The oxirene study was just plain nasty. Results at various levels of theory show differences not just of quantitative accuracy but of the qualitative nature of the stationary point. At the highest levels of theory oxirene is shown to be a true minimum. Experimental confirmation of this hard won fact would be wonderful. Matrix-isolation infrared (IR) spectroscopy is an obvious choice for the laboratory identification of oxirene. However, observation by this technique may be problematic. For example, the vinylidene species with a barrier to isomerization of roughly 2 kcal/mole is well established as a molecular entity by negative-ion photodetatchment spectroscopy but has yet to be observed via matrix-isolation IR spectroscopy. Oxirene has no stable negative-ion, as well, so photodetatchment spectroscopy is not an option.

The high levels of theory used in this work to definitively show oxirene to be a minimum are prohibitively costly for the study of the other (lower-symmetry) structures on the oxirene-ketene isomerization reaction surface or the Wolff-rearrangement reaction surface. We have suggested compromise levels of theory which are both accurate enough and efficient enough for that purpose. Such levels of theory have been taken up by others and lead to fruitful studies of the entire PE hypersurface.[1] Those results clearly support the participation of the oxirene minimum in the Wolff rearrangement. Entry into the rearrangement via formylmethylene will still result in carbon scrambling via oxirene since the energetic barrier to scrambling (oxygen-ring formation and subsequent opening) is much smaller that the 5.5 kcal/mole barrier to (hydrogen transfer) isomerization to ketene.

---

[1] A. P. Scott, R. H. Nobes, H. F. Schaefer and L. Radom, *J. Am. Chem. Soc.* **116**, 10165 (1994).